AD 747234

NRL Memorandum Report 2480

# Fluorescence Amplification and Parasitic Oscillation Limitations in Disc Lasers

JOHN B. TRENHOLME

*Laser Physics Branch*

*Optical Sciences Division*

July 1972

NATIONAL TECHNICAL
INFORMATION SERVICE

NAVAL RESEARCH LABORATORY
Washington, D.C.

Approved for public release; distribution unlimited.

69

UNCLASSIFIED
Security Classification

## DOCUMENT CONTROL DATA - R & D

*Security classification of title, body of abstract and indexing annotation must be entered when the overall report is classified)*

| | |
|---|---|
| 1. ORIGINATING ACTIVITY (Corporate author)<br>Naval Research Laboratory<br>Washington, D.C. 20390 | 2a. REPORT SECURITY CLASSIFICATION<br>UNCLASSIFIED<br>2b. GROUP<br>--- |

3. REPORT TITLE

FLUORESCENCE AMPLIFICATION AND PARASITIC OSCILLATION LIMITATIONS IN DISC LASERS

4. DESCRIPTIVE NOTES (Type of report and inclusive dates)

This is a final report on one phase of the problem; work is continuing on other phases.

5. AUTHOR(S) (First name, middle initial, last name)

John B. Trenholme

| | | |
|---|---|---|
| 6. REPORT DATE<br>July 1972 | 7a. TOTAL NO. OF PAGES<br>70 | 7b. NO. OF REFS<br>11 |
| 8a. CONTRACT OR GRANT NO<br>NRL Problem K03-08.502<br>b. PROJECT NO.<br>ARPA Order 2062<br>c.<br>d. | 9a. ORIGINATOR'S REPORT NUMBER(S)<br>NRL Memorandum Report 2480<br>9b. OTHER REPORT NO(S) (Any other numbers that may be assigned this report) | |

10. DISTRIBUTION STATEMENT

Approved for public release; distribution unlimited.

| | |
|---|---|
| 11. SUPPLEMENTARY NOTES | 12. SPONSORING MILITARY ACTIVITY<br>Advanced Research Projects Agency<br>Washington, D.C. 20310 |

13. ABSTRACT


In disc laser amplifiers, the achievable inversion (and thus the gain and energy output) is limited by fluorescence amplification and parasitic oscillation. In this paper, analytic results and Monte Carlo calculations of both these effects are presented for spheres, circular discs, and elliptical discs. The effects of gain, fluorescence line profile, refractive indices, and disc thickness on fluorescence amplification are presented. The loss rate is seen to increase rapidly above an across-diameter gain of exp (5) or so, independent of thickness. Parasitic oscillation is analyzed as a function of edge and face index ratios, and of edge roughening. Above exp (3) gain, parasitic suppression is difficult, even with a rough edge. Parasitics thus appear to present more difficulties than fluorescence amplification. The effects of both processes on peak inversion achieved during a pumping pulse are also presented. In conclusion, the maximum practical size of $Nd^{3+}$ glass laser discs is estimated to be about 30 cm due to the effects of parasitic oscillation and fluorescence amplification.


DD FORM 1 NOV 65 1473 (PAGE 1)

S/N 0101-807-6801

UNCLASSIFIED
Security Classification

UNCLASSIFIED
Security Classification

| 14 KEY WORDS | LINK A ROLE | LINK A WT | LINK B ROLE | LINK B WT | LINK C ROLE | LINK C WT |
|---|---|---|---|---|---|---|
| Lasers | | | | | | |
| Fluoresence | | | | | | |
| Laser amplifiers | | | | | | |
| Disc lasers | | | | | | |
| Laser parasitic oscillation | | | | | | |
| Laser design | | | | | | |

DD FORM 1 NOV 65 1473 (BACK)
(PAGE 2)

ib

UNCLASSIFIED
Security Classification

## TABLE OF CONTENTS


I. INTRODUCTION ..... 1

II. FLUORESCENCE AMPLIFICATION ..... 2

A. Fluorescence Amplification in a Sphere ..... 4

1. Single-Wavelength Calculation ..... 4

2. Lorentzian Line Profile ..... 8

3. Gaussian Line Profile ..... 12

4. Summary of Analytic Sphere Results ..... 13

5. Monte Carlo Calculation ..... 14

B. Circular Disc ..... 16

1. Analytic Approximation: Thin Disc, Low Gain ..... 16

α. Radiation Below the Critical Angle ..... 18

β. Radiation Above the Critical Angle ..... 24

γ. Total Result ..... 28

2. Monte Carlo Calculation ..... 30

C. Elliptical Disc ..... 35

D. Discussion ..... 37

III. PARASITIC OSCILLATION ..... 40

A. Lossless Modes in a Circular Disc ..... 42

B. Lossy Modes in a Circular Disc ..... 48

C. Combined Oscillation Diagram ..... 51

D. Parasitic Oscillation with a Rough Edge ..... 52

E. Discussion ..... 55

IV. EFFECTS ON PUMPING..... 57

A. Fluorescence Amplification..... 57

B. Parasitic Oscillation..... 60

V. CONCLUSIONS..... 60

## ABSTRACT

In disc laser amplifiers, the achievable inversion (and thus the gain and energy output) is limited by fluorescence amplification and parasitic oscillation. In this paper, analytic results and Monte Carlo calculations of both these effects are presented for spheres, circular discs, and elliptical discs. The effects of gain, fluorescence line profile, refractive indices, and disc thickness on fluorescence amplification are presented. The loss rate is seen to increase rapidly above an across-diameter gain of exp (5) or so, independent of thickness. Parasitic oscillation is analyzed as a function of edge and face index ratios, and of edge roughening. Above exp (3) gain, parasitic suppression is difficult, even with a rough edge. Parasitics thus appear to present more difficulties than fluorescence amplification. The effects of both processes on peak inversion achieved during a pumping pulse are also presented. In conclusion, the maximum practical size of $Nd^{3+}$ glass laser discs is estimated to be about 30 cm due to the effects of parasitic oscillation and fluorescence amplification.



Authorization

NRL Problem K03-08.502

Project No. ARPA Order 2062


This is a final report on one phase of the problem; work is continuing on other phases.

## I. INTRODUCTION

Multi-disc laser amplifiers are presently of interest in the production of high-energy light pulses for the generation of dense, high-temperature plasmas for x-ray generation and controlled thermonuclear reactions. Disc amplifiers, as compared to rod amplifiers, have the advantages of more uniform pumping, easy heat removal, small size of individual glass pieces, and less susceptibility to self-trapping. However, the design of these amplifiers must be carefully carried out if costly and time-consuming mistakes are not to be made.

One of the problems which must be understood before disc amplifier design is undertaken is that of fluorescence amplification[1-9] (sometimes called amplified spontaneous emission, superfluorescence, or - incorrectly[10] - superradiance). Fluorescence amplification makes energy storage in lasers more and more difficult as the inversion level rises. Section II of this paper is a discussion of analytical and Monte Carlo calculations of the limitations due to fluorescence amplification in various geometrical shapes relevant to the disc laser problem, and of the effects of varying size, shape, gain, refractive index, and line profile.

Another problem which arises in disc amplifier design is parasitic oscillation. Such oscillation sets a sharp upper limit to the achievable inversion, and often is a more serious problem than fluorescence amplification. In Section III of this paper, parasitic oscillation limits to achievable gain in a single disc will be calculated as a function of the reflections due to the refractive indices of a disc and its surroundings, and as a function of the edge roughness of the disc.

Both fluorescence amplification and parasitic oscillation act to limit the maximum practical size of the discs in a disc amplifier, since both processes get worse as a disc becomes larger (assuming constant inversion density). Accurate analysis of both effects is therefore required to determine the exact limitations on size and gain.

## II. FLUORESCENCE AMPLIFICATION

Many materials, when properly pumped, exhibit fluorescence (the spontaneous emission of photons). The fluorescence arises when the upper level of the fluorescent transition is populated by the pumping process, and radiative transitions to the lower level take place. Once the pumping is turned off the fluorescence usually decays exponentially with a time constant called the fluorescent lifetime $\tau$. An exponential decay implies that the process is linear - that is, that the fluorescence is linearly proportional to the population in the upper level.

Suppose, however, that the pumping was so intense that an inversion exists; the population in the upper level is greater than the population in the lower level. The pumped material then exhibits optical gain at the transition frequency, and may be used to amplify light in a laser amplifier or oscillator. However, the fluorescence continues under conditions where gain exists; in fact, the processes of spontaneous emission (fluorescence) and stimulated emission (gain) are inextricably interconnected. This means that fluorescent light, once emitted within the volume of the material, will be amplified before it reaches the edges. This increases the effective fluorescence loss rate, which is the same as decreasing the instananeous

fluorescent lifetime. Because the gain, and thus the added loss, now depends on the inversion level, the fluorescent decay process is no longer linear. Instead, the decay rate becomes faster as the inversion level increases. This fluorescence amplification problem is especially severe in large laser systems, since the long path lengths available lead to large total gain and thus large amounts of fluorescence amplification.

So far we have considered what happens when the pumping is over. However, the fluorescence and gain processes also exist during the pump pulse. If the fluorescence amplification is negligible, so that the system is linear, then doubling the pumping amplitude will double the inversion. In general, the peak inversion will be linearly proportional to the pump pulse amplitude. This proportionality will be destroyed if gain exists in the material. In the presence of fluorescence amplification, equal increments of pumping will yield smaller and smaller inversion (and gain) increases, because the decay rate per unit of inversion will increase with the inversion. The details of pumping in the presence of fluorescence amplification are studied in Section IV.

In this section we will consider only single-pass fluorescence amplification. That is, the edges of the discs will be assumed to be totally absorbing, so that once the fluorescent light hits an edge it is not reflected back into the disc again. This is the best possible edge condition for an amplifier, since if the disc edge is not perfectly black the light will be reflected back into the disc and excite further stimulated emission, thus increasing the fluorescence loss rate. We are therefore

calculating an upper bound on gain due to the effects of fluorescence amplification, since any actual disc will return some reflected light, thus increasing the loss rate and decreasing the gain. We here limit ourselves to the black-edge case because once light is reflected from the edges oscillation will occur at some gain level and a different method of analysis must be used to find this level (see Section III).

## A. Fluorescence Amplification in a Sphere

We first calculate the stimulated emission in a sphere, not because sphere lasers[11] are of interest but because an exact analytical calculation is possible in this case. In addition, the sphere forms a simple system in which to demonstrate the effects of line shape.

### 1. Single-Wavelength Calculation

Consider a laser material in the shape of a sphere. We will assume that a spatially uniform inversion exists throughout the sphere, and make a calculation of the instantaneous rate of fluorescence amplification. The inversion causes the material to have a gain coefficient $\alpha$, such that the intensity of a pencil of light rays increases as $P = P_o \exp(\alpha \ell)$, where $\ell$ is the path length along the ray direction. Suppose that spontaneous emission releases a power of I per unit volume. If the sphere has a diameter D, the total spontaneous emission is $I \pi D^3/6$. We will calculate the amount by which this spontaneous emission is amplified.

Introduce a system of spherical coordinates centered on the surface of the sphere (Fig. 1). The angle $\phi$ is measured from the sphere diameter, and $\theta$ gives the rotation around the diameter. The distance r is measured

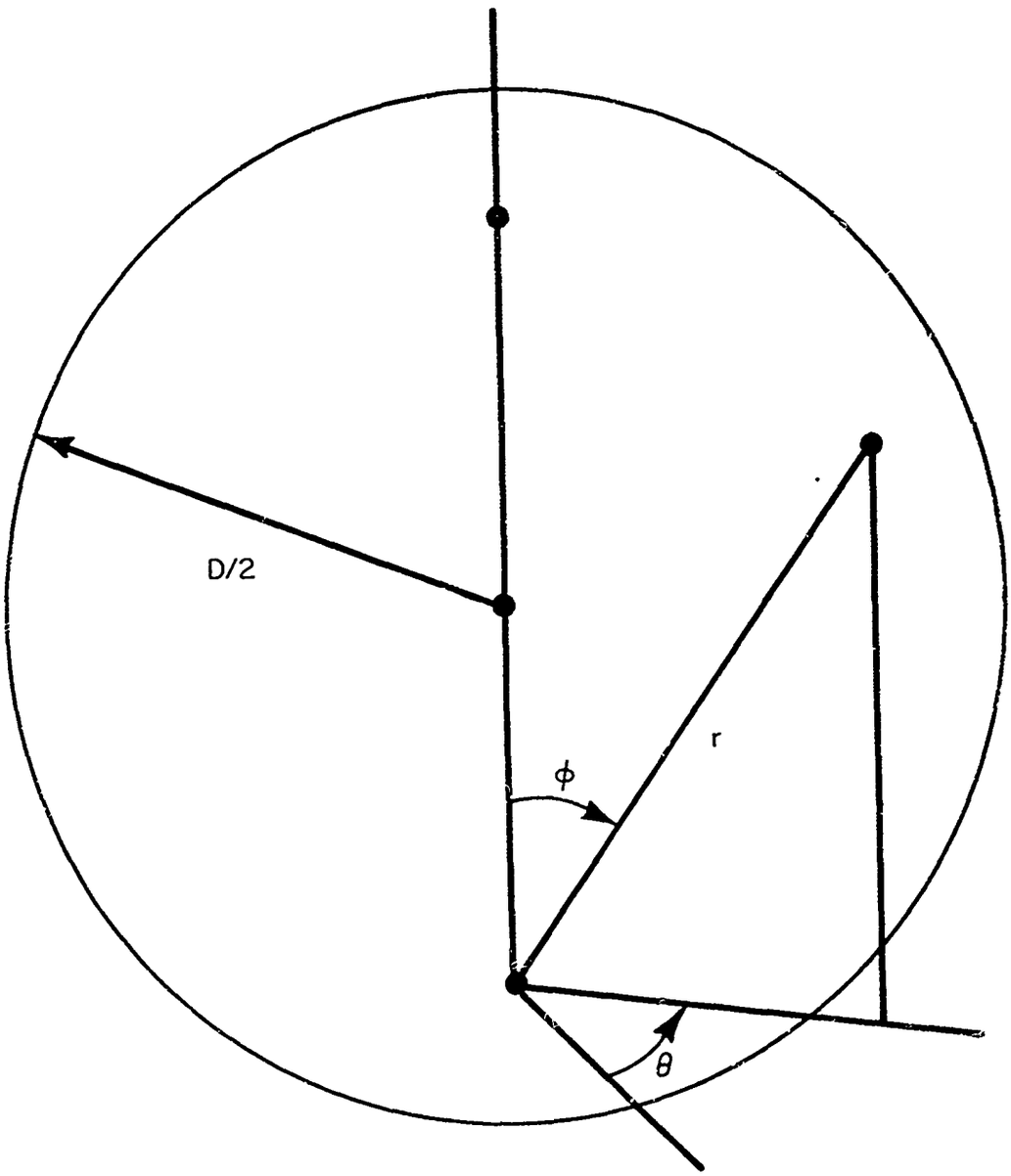


Fig. 1 - Coordinate system for the analysis of fluorescence amplification in a sphere of diameter D. The origin is at the sphere's south pole.

along the direction defined by $\theta$ and $\phi$. The element of volume in these coordinates is $r^2 \sin\phi \, dr \, d\theta \, d\phi$, and the fluorescence from this volume is $I \, r^2 \sin\phi \, dr \, d\theta \, d\phi$. We assume that this fluorescence is emitted isotropically. An element of sphere surface of area dS at the origin of coordinates will intercept a fraction of the fluorescence equal to the projected area of dS in the direction of the volume element ($dS \cos\phi$) divided by the area of a sphere centered on the volume element and passing through the origin ($4 \pi r^2$). However, the fluorescence will be amplified by a factor exp ($\alpha r$) before it reaches dS. Thus dS will intercept a total radiation (spontaneous plus stimulated) of

$$\frac{I}{4\pi} \exp(\alpha r) \cos\phi \sin\phi \, dr \, d\theta \, d\phi \, dS.$$

Now integrate this expression over the volume of the sphere to find the total flux on the area dS:

$$dP = \frac{I \, dS}{4\pi} \int_0^{2\pi} d\theta \int_0^{\pi/2} d\phi \int_0^{D\cos\phi} dr \, e^{\alpha r} \cos\phi \sin\phi$$

$$= \frac{I \, dS}{2} \int_0^{\pi/2} d\phi \int_0^{D\cos\phi} dr \, e^{\alpha r} \cos\phi \sin\phi$$

$$= \frac{I \, dS}{2\alpha} \int_0^{\pi/2} d\phi \left( e^{\alpha D\cos\phi} - 1 \right) \cos\phi \sin\phi \quad .$$

With the change of variable $u = \cos\phi$, the flux becomes

$$dP = \frac{I\ dS}{2\alpha} \int_0^1 du\ u \left(e^{\alpha D u} - 1\right)$$

$$= \frac{I\ ds}{2\alpha} \left\{ e^{\alpha D} \left[ \frac{1}{\alpha D} - \frac{1}{(\alpha D)^2} \right] + \frac{1}{(\alpha D)^2} - \frac{1}{2} \right\} .$$

By symmetry, all elements of the sphere surface receive the same flux, so the total emission hitting the sphere surface is

$$P = \frac{I\ \pi\ D^2}{2\alpha} \left[ \frac{e^{\alpha D}}{\alpha D} \left(1 - \frac{1}{\alpha D}\right) + \frac{1}{(\alpha D)^2} - \frac{1}{2} \right] .$$

To find the amount M by which the original spontaneous emission has been multiplied, divide by the total spontaneous emission $I\ \pi\ D^3/6$ and find

$$M = \frac{3}{2\beta} \left[ \frac{2e^{\beta}}{\beta} \left(1 - \frac{1}{\beta}\right) + \frac{2}{\beta^2} - 1 \right] ,$$

where we have introduced the variable $\beta = \alpha D$. Note that $\beta$ is the log of the gain straight across the sphere. The ratio of stimulated to spontaneous emission is

$$A = \frac{3}{2\beta} \left[ \frac{2e^{\beta}}{\beta} \left(1 - \frac{1}{\beta}\right) + \frac{2}{\beta^2} - 1 \right] - 1 .$$

Our calculation has been for a single value of $\alpha$. However, in actual laser materials the fluorescence and gain are distributed in wavelength according to some line profile, with values from zero to the peak value being represented. The effective values of the spontaneous emission multiplier M and the stimulated-spontaneous ratio A are therefore found by averaging the single wavelength values over the line. From the viewpoint of fluorescence amplification, the worst possible case would be a flat-topped or rectangular line profile, since in that case the line average is equal to the peak value. For more realistic line profiles, in which values less than the peak are represented, the line average is less than the peak $\alpha$ by an amount which depends on the line shape.

It should be noted that $M = 1 + A$ for any line shape, since by definition $M = (J + K)/J = 1 + J/K$ and $A = J/K$, where J is the spontaneous radiation and K is the stimulated radiation.

2. Lorentzian Line Profile

Let us, for example, calculate the values of M and A for a Lorentzian line profile. The gain (and the fluorescence, which has the same line shape) have the form

$$\alpha = \frac{\alpha_p}{1 + \frac{2(\lambda - \lambda_o)}{W}^2} .$$

where $\alpha_p$ is the gain at the peak of the line, $\lambda_o$ is the center wavelength and W is the full width at half maximum.

Since all that matters when averaging over a line is the fraction of the line representing different values of $\alpha$, we need to find a function which gives this amplitude weighting. For any symmetric shape of $\alpha$, we have

$$M = \frac{\int_{-\infty}^{+\infty} \alpha\, M\, d\lambda}{\int_{-\infty}^{+\infty} \alpha\, d\lambda}$$

$$= \frac{\int_{0}^{\alpha_p} \alpha\, M \frac{d\lambda}{d\alpha}\, d\alpha}{\int_{0}^{\alpha_p} \alpha \frac{d\lambda}{d\alpha}\, d\alpha} \quad .$$

Introducing the variable $x = \alpha/\alpha_p$, we have

$$M = \int_{0}^{1} M\,(\alpha_p)\ \rho_L(x)\ dx$$

where the Lorentzian weighting function $\rho_L(x)$ is given by

$$\rho_L(x) = \frac{\alpha \frac{d\lambda}{d\alpha}}{\int_{0}^{\alpha_p} \alpha \frac{d\lambda}{d\alpha}\, d\alpha}$$

$$= \frac{\frac{1}{\sqrt{x(1-x)}}}{\int_{0}^{1} \frac{dx}{\sqrt{x(1-x)}}} \quad .$$

Since the integral in the denominator is the beta function $B(\frac{1}{2},\frac{1}{2}) = \pi$, we have

$$\rho_L(x) = \frac{1}{\pi\sqrt{x(1-x)}} \quad .$$

The line-averaged value of the stimulated/spontaneous ratio is given by

$$A_L = \int_0^1 A\left(\alpha_p x\right) \rho_L(x)\, dx$$

$$= \frac{3}{2\pi}\int_0^1 dx \left[\frac{2e^{\beta x}}{\beta^2 x^2}\left(1 - \frac{1}{\beta x}\right) + \frac{2}{\beta^3 x^3} - \frac{1}{\beta x}\right] \frac{1}{\sqrt{x(1-x)}}$$

where $\beta = \alpha_p D$. Unfortunately, the various terms of the integrand lead to (cancelling) infinities. We therefore calculate $A_L$ by a less direct method.

Firstly, we determine the power series expansion of A by expanding the exponential and combining terms. We find

$$A = \frac{3\beta_\lambda}{8} + \frac{\beta_\lambda^2}{10} + \frac{\beta_\lambda^3}{48} + \frac{\beta_\lambda^4}{280} + \ldots\ldots.$$

$$= \sum_{n=1}^{\infty} \frac{3\beta_\lambda^{\,n}}{(n+3)(n+1)!}$$

where $\beta_\lambda = \alpha D$.

Then the line average is

$$A_L = \frac{3}{\pi} \int_0^1 dx \left[ \sum_{n=1}^{\infty} \frac{\beta^n x^{n-\frac{1}{2}}}{(1-x)^{\frac{1}{2}} (n+3)(n+1)!} \right] .$$

We reverse the order of summation and integration, and use the fact that the integral over x is a beta function to find

$$A_L = \frac{3\beta}{16} + \frac{3\beta^2}{80} + \frac{5\beta^3}{768} + \frac{\beta^4}{1024} + \ldots\ldots$$

$$= \sum_{n=1}^{\infty} \left[ \frac{3\beta^n}{(n+3)(n+1)!} \prod_{r=1}^{n} \left( \frac{2r-1}{2r} \right) \right] .$$

Since the series must be summed numerically to find the $A_L$ corresponding to some specific $\beta$, the error due to truncating at any n must be known. Let the relative error due to ignoring terms beyond m be $\epsilon_n$, so that

$$A_L = \left( \sum_{n=1}^{m} a_n \beta^n \right) \left( 1 + \epsilon_m \right)$$

where

$$a_n = \frac{3}{(n+3)(n+1)!} \prod_{r=1}^{n} \left( \frac{2r-1}{2r} \right) .$$

Then we have

$$\epsilon_m = \left(\sum_{n=m+1}^{\infty} a_n\beta^n\right) \Big/ \left(\sum_{n=1}^{m} a_n\beta^n\right) \quad .$$

As m becomes large, the ratio of successive coefficients of $\beta$ in the expansion of $A_L$ becomes

$$\frac{a_{n+1}}{a_n} = \frac{(n+3)(2n+1)}{(n+4)(n+2)(2n+2)} \rightarrow \frac{1}{n + \frac{7}{2}} \quad .$$

We therefore have an upper limit to the truncated part of the series:

$$\sum_{n=m+1}^{\infty} a_n\beta^n < \sum_{n=0}^{\infty} a_{m+1}\beta^{m+1}\left(\frac{\beta}{m+9/2}\right)^n = \frac{a_{m+1}\beta^{m+1}}{1 - \frac{\beta}{m+9/2}} \quad .$$

Therefore

$$\epsilon_m < \frac{a_{m+1}\beta^{m+1}}{\left(1 - \frac{\beta}{m}\right)\sum_m}$$

where $\sum_m = \sum_{n=1}^{m} a_n\beta^n$.

3. Gaussian Line Profile

We may find the effect of a Gaussian line profile having the form

$$\alpha = \alpha_p \, 2^{-4\left(\frac{\lambda-\lambda_o}{W}\right)^2}$$

by the same method used for the Lorentzian line. In this case, the amplitude weighting function is

$$\rho_G(x) = \frac{1}{\sqrt{-\pi \ln x}}$$

and term-by-term integration of the series expansion of A yields

$$A_G = \frac{3\beta}{8\sqrt{2}} + \frac{\sqrt{3}\,\beta^2}{30} + \frac{\beta^3}{96} + \frac{\beta^4}{280\sqrt{5}} = \ldots\ldots$$

$$= \sum_{n=1}^{\infty} \frac{3\beta^n}{(n+3)(n+1)!\,\sqrt{n+1}} \quad .$$

In this case, as in the Lorentzian one, the ratio of successive coefficients approaches $n + 7/2$ as $n \to \infty$, and so the truncation error limit given for the Lorentzian line profile also applies to the series expansion of A for a Gaussian line profile.

4. Summary of Analytic Sphere Results

Table I gives numerical values of the ratio of stimulated to spontaneous radiation A as a function of $\beta$ (the log of the across-sphere gain at the line peak) for flat-topped, Gaussian, and Lorentzian line profiles of the gain coefficient. For small values of $\beta$, we see that A is linearly dependent on $\beta$ with a coefficient which depends on the line shape. The rise of A with $\beta$ becomes faster as $\beta$ approaches unity, and is very fast for values of $\beta$ much greater than one. We shall see later that this behavior is typical of any shape of laser material. The fact that decay rates rise sharply for $\beta > 1$ means that pumping becomes more and more difficult in this region.

TABLE I

Ratio of stimulated to spontaneous radiation A in a sphere as a function of the log of the across-sphere gain at the line peak $\beta$ for flat-topped, Gaussian, and Lorentzian line profiles.

| $\beta$ | $A_{FLAT}$ | $A_{GAUSS}$ | $A_{LORENT}$ |
|---|---|---|---|
| .01 | .003760 | .002657 | .001879 |
| .02 | .007540 | .005326 | .003765 |
| .05 | .01900 | .01340 | .009470 |
| .1 | .03852 | .02710 | .01913 |
| .2 | .07917 | .05543 | .03905 |
| .5 | .2153 | .1484 | .1040 |
| 1. | .5000 | .3352 | .2326 |
| 2. | 1.396 | .8790 | .5980 |
| 5. | 12.97 | 6.497 | 4.153 |
| 10. | 593.6 | 206.8 | 123.4 |
| 20. | $3.457 \times 10^{6}$ | $8.097 \times 10^{5}$ | $4.670 \times 10^{5}$ |
| 50. | $6.097 \times 10^{18}$ | $8.778 \times 10^{15}$ | $4.992 \times 10^{17}$ |
| 100. | $7.984 \times 10^{39}$ | $8.055 \times 10^{38}$ | $4.562 \times 10^{38}$ |

## 5. Monte Carlo Calculation

The amount of fluorescence amplification in a sphere was also calculated by means of a Monte Carlo optical power flow program. Since analytical results are available in the case of a sphere, it may seem pointless to duplicate the results with an approximate method. However, the Monte Carlo

program can be used with geometric shapes of arbitrary complexity. Thus it is much more general in its application than analytic methods, but of course any such program should be checked in a geometry where the results are known. This is the reason for its use in the case of a sphere.

The Monte Carlo program is called ZAP. It traces optical power flow in systems which are made up of segments bounded by planes, spheres, cylinders, cones, conic surfaces, and so forth, or in combinations of such segments. The material in the segments is specified by its refractive index and absorption (or amplification) coefficient. The system surfaces may have constant or angle-varying reflection, both specular and scattering. Each optical ray carries with it up to two hundred wavelength intervals. The bulk and surface properties of the system may vary with wavelength, and the optical power in each wavelength interval will change according to the system properties at its particular wavelength. Rays are started at random from specified sources (surface or volume) with given initial wavelength distributions of power, and traced through the system to find the deposition or extraction of power in all the system elements. A ray cut-off scheme is used which assures that ray truncation error is small without wasting time following weak rays. ZAP was designed for accurate modelling of laser pump cavities (a job it does well), but it is also well suited to the calculation of fluorescence amplification in arbitrary geometries.

The sphere geometry was specified to ZAP, and runs of 2500 rays were made for various values of $\beta$ to achieve an accuracy of two or three percent. The rays were started at random throughout the sphere, to correspond to uniform inversion. All rays hitting the sphere surface were totally absorbed.

Runs were made for a flat-topped line (one wavelength), for a line with a Gaussian profile, and for a line with a Lorentzian profile. The Gaussian and Lorentzian lines were modelled by dividing a line profile into equal intervals of wavelength. The gain coefficient and starting power in each wavelength interval were then taken proportional to the value of the gain coefficient at the center of the interval. It is necessary to go a large distance out on the tail of the Lorentzian line in order to get a proper weighting of low values of the gain (recall that the Lorentzian amplitude weighting function approaches infinity as the amplitude approaches zero). The final result, with the above number and spacing of wavelengths, is about 1% high for a sphere when the calculation is exact. To this systematic error, the Monte Carlo method adds the previously mentioned random error of 2 or 3%.

A comparison of the analytic and Monte Carlo results for a sphere is shown in Fig. 2. The agreement is quite satisfactory, since the exact result lies within the Monte Carlo error limits in all cases.

B. Circular Disc

We will now consider the case of a circular disc, which is of considerably greater practical interest. We will first perform an approximate analytic calculation which is exact for infinity thin discs at low gain, and then find the results for thick discs and/or high gain by the Monte Carlo method.

1. Analytic Approximation: Thin Disc, Low Gain

Consider the spontaneous fluorescence emitted from a small element of volume in a circular disc with a totally absorbing edge. Some of the radiation will strike the edge directly, while the rest will hit the faces. Both components will be amplified as they travel. The radiation which goes to

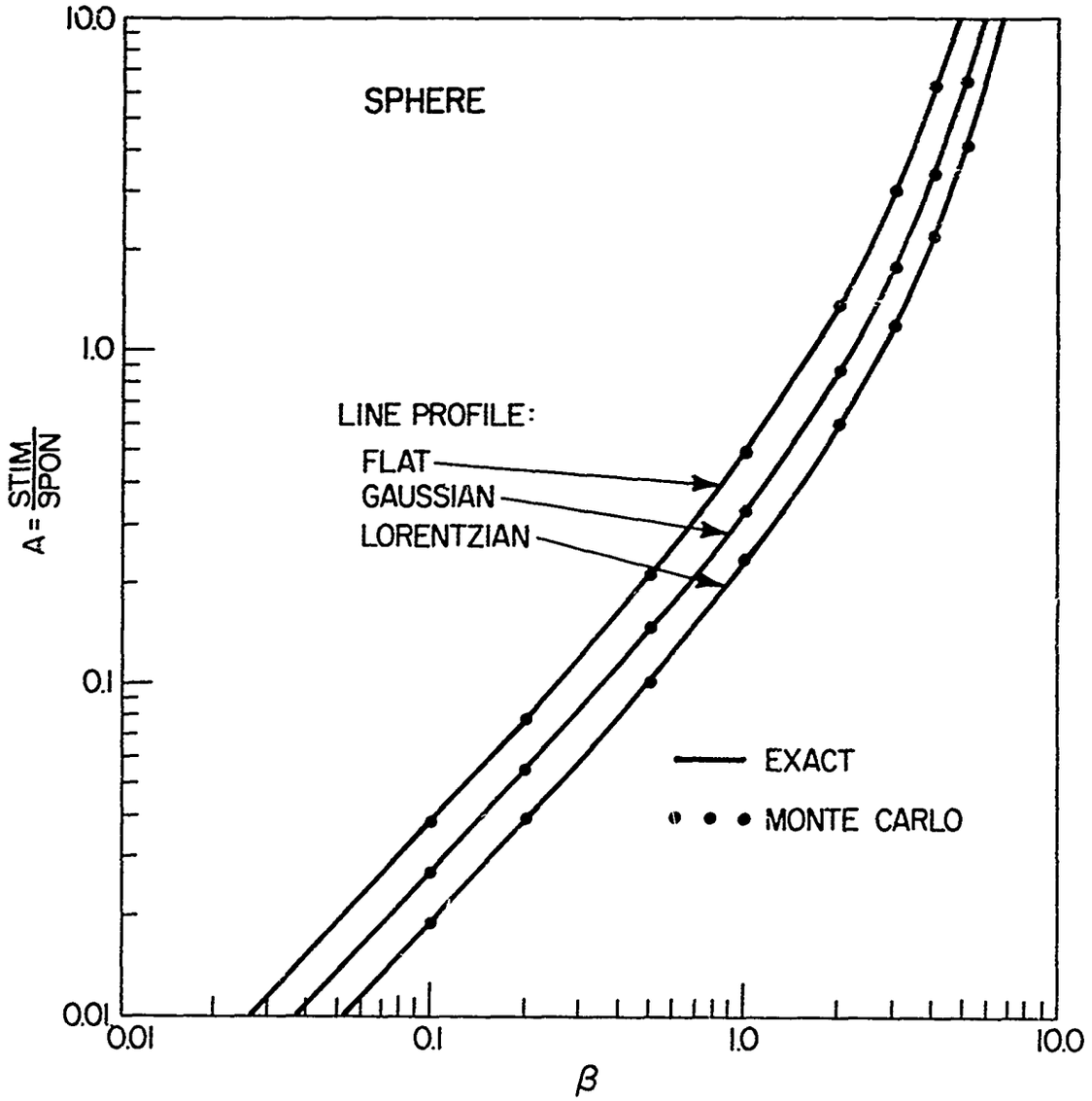


Fig. 2 - Analytic and Monte Carlo values for the ratio A of stimulated to spontaneous loss as a function of the product β of the gain coefficient and diameter for a sphere. Curves are shown for three different line profiles of the gain coefficient.

the faces can be further separated into two parts. Some will strike at less than the critical angle for total internal reflection, in which case most will be transmitted and a small fraction ($\sim 5\%$) reflected back into the disc. Some will strike at more than the critical angle, and will be totally reflected back into the disc. This totally reflected component will continue to bounce back and forth between the faces until it finally strikes the black edge. The path length for this process is the same as if the radiation had gone straight to the continuation of the edge beyond the faces (Fig. 3). Thus there are two parts of the circular disc gain calculation: the radiation below the critical angle, and that above the critical angle.

α. Radiation below the critical angle

Consider a circular disc of diameter D and thickness L. A volume element at a distance r from the disc center emits a pencil of radiation at an angle $\phi$ from the normal to the disc (Fig. 4). The distance from the point of emission to the edge is $\ell$; the ray travels a distance $\ell \csc \phi$ before it hits the edge. Note that this result is independent of the position along an axis normal to the disc faces (the z-position) of the emitter. The distance $\ell$ depends on the angle $\theta$ from a disc radius through the emitting element to the emitted pencil. From Fig. 5 we see that

$$\ell = \sqrt{\left(\frac{D}{2}\right)^2 - (r \sin \theta)^2} - r \cos\theta \ .$$

The radiation is multiplied by a factor of exp ($\alpha \ \ell \csc \phi$) as it travels to the edge; we recall that $\alpha$ is the gain coefficient in the material.

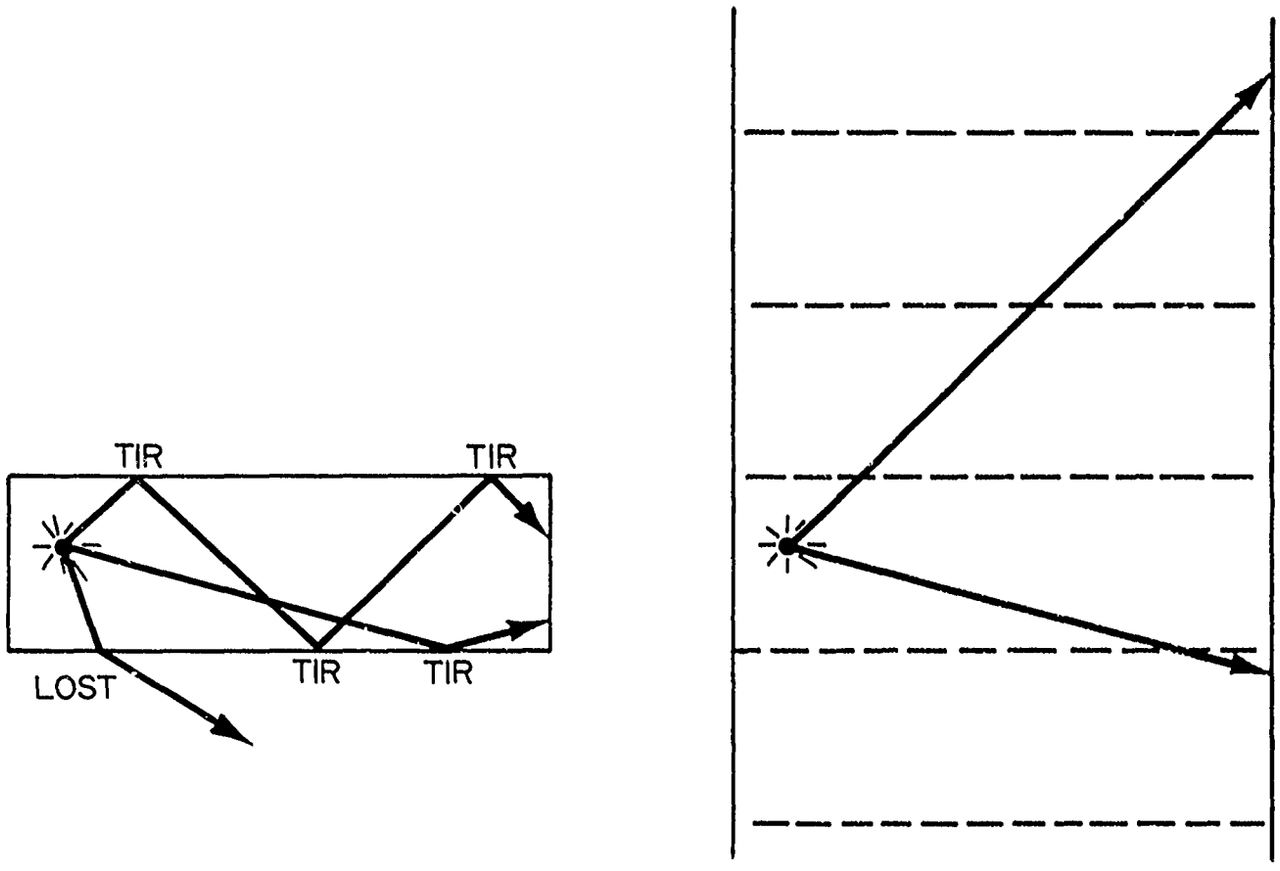


Fig. 3 - Side view of paths of rays which are trapped by total internal reflection in a circular disc. The paths are equivalent to straightline paths in an infinite cylinder, formed by multiple reflections of the disc in its faces.

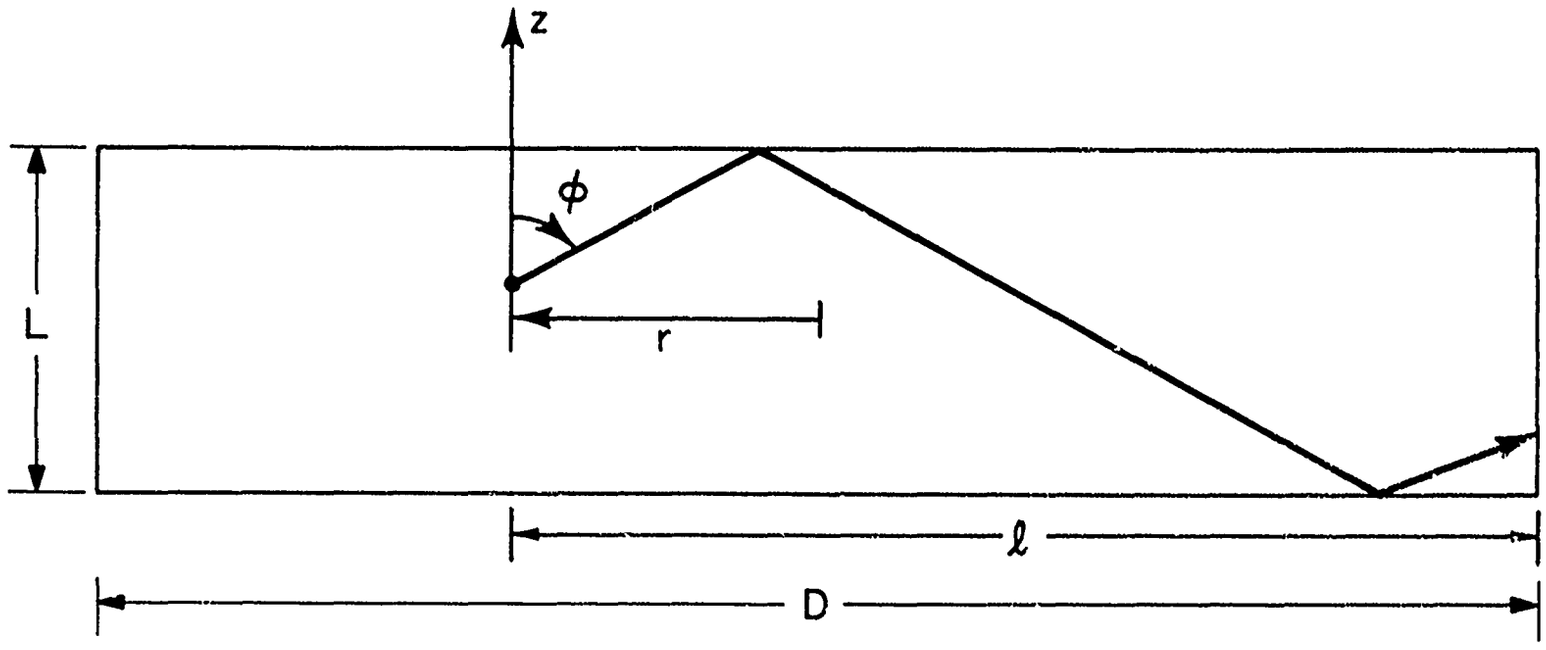


Fig. 4 - Details of the path of a ray which is trapped by total internal reflection in a circular disc. See text.

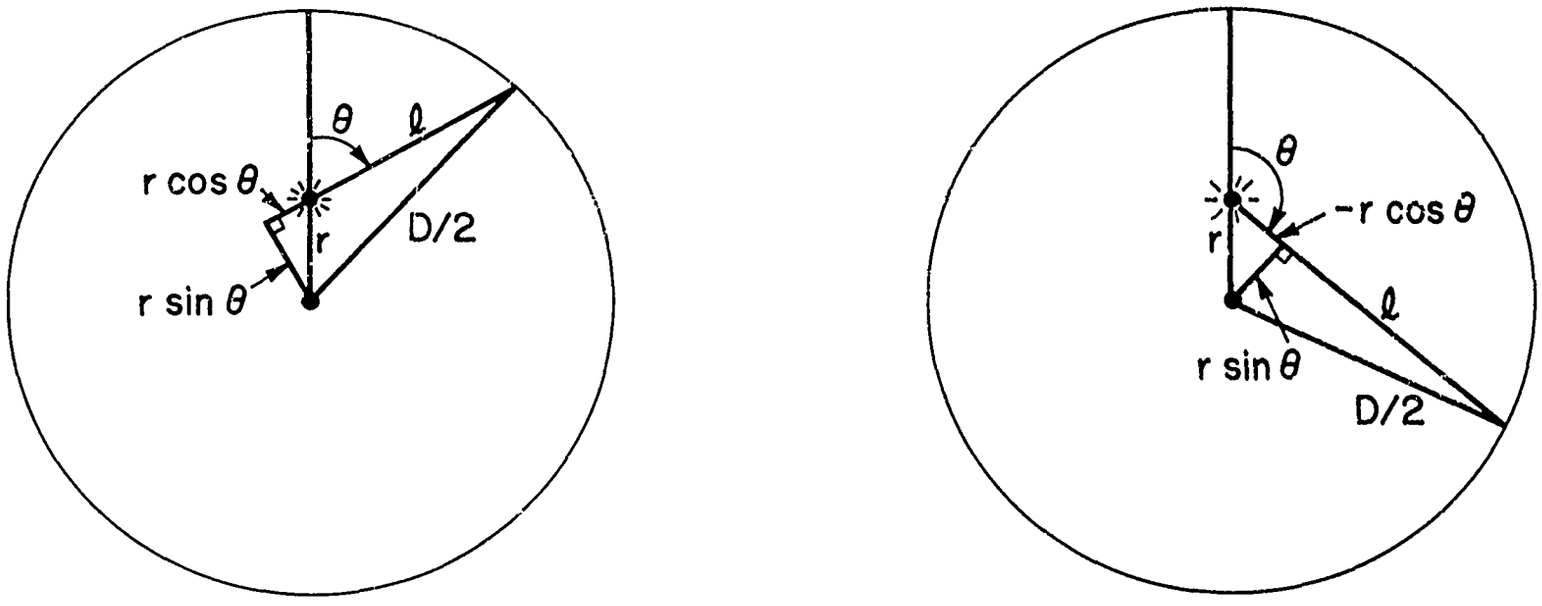


$$(r\cos\theta + \ell)^2 + (r\sin\theta)^2 = (D/2)^2$$

$$\ell = \sqrt{(D/2)^2 - (r\sin\theta)^2} - r\cos\theta$$

Fig. 5 - Geometry for the calculation of the distance from the point of emission to the disc edge. The formula is the same for $\theta < \pi/2$ and $\theta > \pi/2$, as shown.

We must integrate over the disc volume (i.e., over r) and over solid angle. The fractional disc volume at radius r is $8r\,D^{-2}\,dr$, and the fraction of solid angle at $\theta$, $\phi$ is $(4\pi)^{-1}\sin\phi\,d\theta\,d\phi$. The angle $\phi$ varies from $\theta_c$ to $\pi-\theta_c$, where $\theta_c$ is the critical angle, but by symmetry we can take twice the integral from $\theta_c$ to $\pi/2$. Likewise we may take twice the integral from 0 to $\pi$ for $\theta$. The above-critical-angle integral for the ratio M of total to spontaneous emission is then

$$M_1 = \frac{8}{\pi D^2}\int_0^{D/2} dr \int_{\theta_c}^{\pi/2} d\phi \int_0^{\pi} d\theta\; r \sin\phi \exp\left[\frac{\alpha\left(\sqrt{\frac{D^2}{4} - r^2\sin^2\theta} - r\cos\theta\right)}{\sin\phi}\right].$$

This is somewhat clarified by use of the dimensionless variable $u = 2\,r/D$, whence

$$M_1 = \frac{2}{\pi}\int_0^{1} du \int_{\theta_c}^{\pi/2} d\phi \int_0^{\pi} d\theta\; u \sin\phi \exp\left[\frac{\alpha D\left(\sqrt{1 - u^2\sin^2\theta} - u\cos\theta\right)}{2\sin\phi}\right].$$

For the low gain condition $\alpha D \ll 1$, we can expand the exponential in its power series and produce a simpler integral:

$$M_1 = \frac{2}{\pi}\int_0^{1} du \int_{\theta_c}^{\pi/2} d\phi \int_0^{\pi} d\theta\; u \sin\phi \left[1 + \frac{\alpha D\left(\sqrt{1 - u^2\sin^2\theta} - \cos\theta\right)}{2\sin\phi} \pm \ldots\right].$$

The first term in the series yields the simple result $\cos\theta_c$, but the second term is more difficult. Sin $\phi$ cancels in numerator and denominator, so the $\phi$ integral is just $(\pi/2 - \theta_c)$, leaving

$$M_1 = \cos\theta_c + \frac{\alpha D}{\pi}\left(\frac{\pi}{2} - \theta_c\right)\int_0^1 du \int_0^\pi d\theta\, u\left(\sqrt{1 - u^2 \sin^2\theta} - u\cos\theta\right).$$

In the $\theta$ integral, the $\cos\theta$ portion integrates to zero, leaving twice the complete elliptic integral of the second kind

$$2E\left(u^2\right) = \int_0^\pi d\theta\left(\sqrt{1 - u^2 \sin^2\theta}\right).$$

so that

$$M_1 = \cos\theta_c + \frac{2\alpha D}{\pi}\left(\frac{\pi}{2} - \theta_c\right)\int_0^1 du\, u\, E\left(u^2\right)$$

which by the change of variable $q = u^2$ becomes

$$M_1 = \cos\theta_c + \frac{\alpha D}{\pi}\left(\frac{\pi}{2} - \theta_c\right)\int_0^1 dq\, E(q)$$

thus yielding the final result

$$M_1 = \cos\theta_c + \frac{\alpha D}{\pi}\left(\frac{\pi}{2} - \theta_c\right)\left(\tfrac{1}{2} + G\right) \pm \ldots$$

where $G = .9159656 \cdots$ is Catalan's constant.

## β. Radiation above the critical angle

Let us follow the radiation emitted at above the critical angle for total internal reflection by a volume element at distance b from the disc face (Fig. 6). Starting at angle $\phi$ from the normal to the face, the ray travels a distance b sec $\phi$ before it hits the face. The relative strength is now exp ($\alpha$ b sec $\phi$). A fraction T is transmitted through the face and (for our purposes) lost, while (1-T) is reflected and crosses the disc. The path length to the opposite face is L sec $\phi$ (recall that L is the disc thickness), and so the reflected ray is amplified by exp ($\alpha$ L sec $\phi$). It then again loses a fraction T to the outside, and (1-T) recrosses the disc, is amplified, and is partially transmitted and partially reflected. The bouncing process continues until the ray hits an absorbing edge. Let the relative strength at the first encounter of the face be P = exp ($\alpha$ b sec $\phi$), and define the gain on a pass all the way across the disc to be K = exp ($\alpha$ L sec $\phi$). Then the ray strength is as follows (Fig. 7):

| | |
|---|---|
| 1 | at the start |
| P | at the initial face intercept |
| P(1-T) | after the first reflection |
| P(1-T)K | after crossing to the opposite face |
| $P(1-T)^2K$ | after the second reflection |
| $P(1-T)^2K^2$ | after the second full crossing |
| $P(1-T)^3K^2$ | after the third reflection |
| $P(1-T)^3K^3$ | after the third full crossing |

and so forth. The total amount radiated is then $PT + PT(1-T)K + PT(1-T)^2K^2 + PT(1-T)^3K^3 + \ldots$ which sums to $PT/[1 - (1-T)K]$ if we take an infinite number

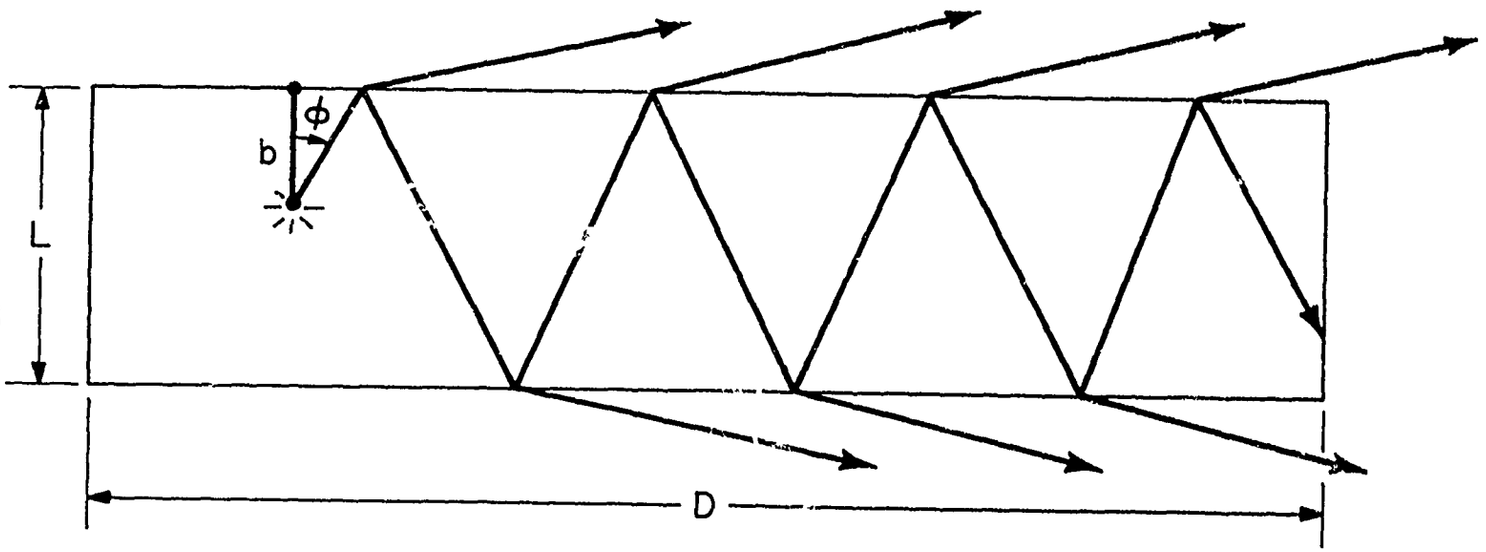


Fig. 6 - Path of a ray which is partially transmitted at the disc faces. The ray bounces from face to face, losing energy to the exterior on each reflection.

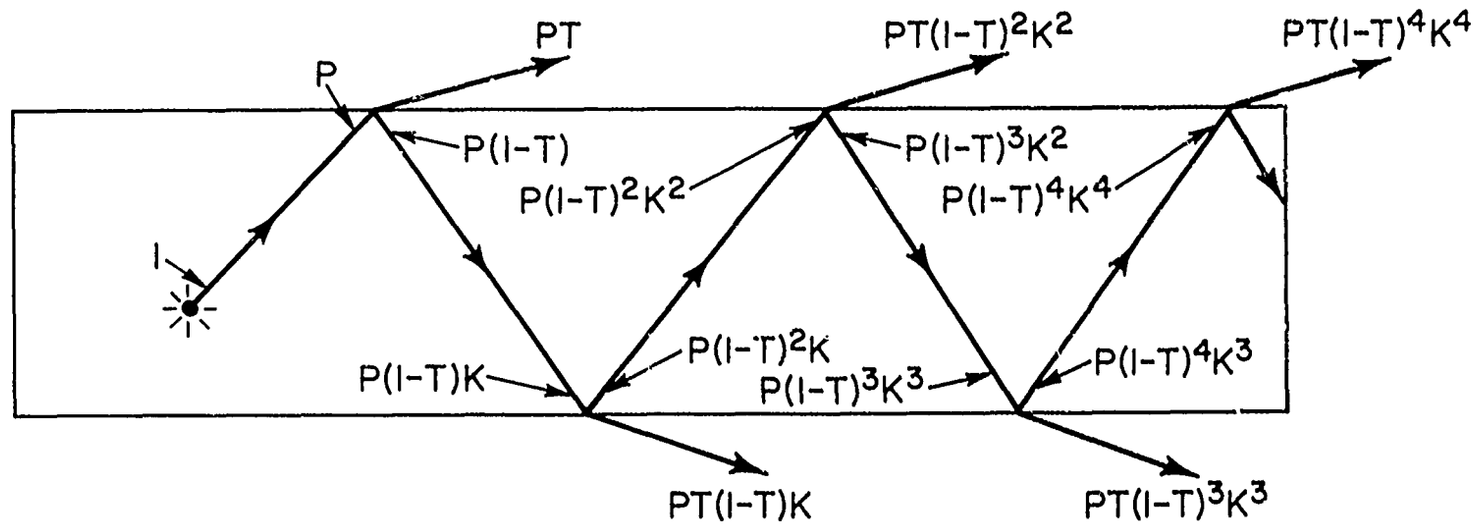


Fig. 7 - Amount of power in a partially reflected ray as a function of position. P is the power at the first reflection, T is the transmitted fraction at the surface, and K is the gain across the disc. See text.

of terms. Of course, the actual ray will terminate after a finite number of bounces, but the error in the infinite-bounce approximation is small as long as the gain across the disc times the reflectivity is small, in which case the ray strength is reduced to a negligible value in just a few bounces. This small-gain case is exactly the one we are calculating, so we will use the infinite-bounce approximation above, which overestimates the actual result.

We must integrate over angle and position to find the overall average gain. The fractional solid angle at angle $\phi$ is $\sin\phi\, d\phi/2$, and the fractional volume is $db/L$ (note that the r and $\theta$ integrals have vanished because there is no r or $\theta$ dependence in the infinite-bounce approximation). Then the above-critical-angle radiation contributes approximately

$$M_2 \cong \frac{1}{L}\int_0^{\theta_c} d\phi \int_0^L db \; \frac{T \exp(\alpha\, b \sec\phi) \sin\phi}{1 - (1-T)\exp(\alpha\, L \sec\phi)}$$

where we have (by symmetry) taken twice the $\phi$ integral from 0 to $\theta_c$ rather than the integral from 0 to $\theta_c$ plus the integral from $\pi - \theta_c$ to $\pi$. For $\alpha L \ll 1$ we expand the exponentials in the integrand and divide to get

$$M_2 \cong \frac{1}{L}\int_0^{\theta_c} d\phi \int_0^L db \; \sin\phi \left(1 + \frac{\alpha b}{\cos\phi} + \frac{(1-T)\,\alpha L}{T\cos\phi} \pm \ldots\right)$$

$$= \int_0^{\theta_c} d\phi \; \sin\phi \left(1 + \frac{\alpha L\left(\frac{1}{T} - \frac{1}{2}\right)}{\cos\phi} \pm \ldots\right)$$

which integrates to

$$M_2 \cong \left(1 - \cos\theta_c\right) + \alpha L \left(\frac{1}{T} - \frac{1}{2}\right) \ln\left(\frac{1}{\cos\theta_c}\right) \pm \ldots \quad .$$

While performing this calculation we have made another approximation: we have assumed that the transmission T is independent of angle, and have ignored the fact that T depends on polarization. In actual fact, T decreases as $\phi$ approaches the critical angle, and more radiation returns to the disc to be amplified. If we use the normal-incidence value for T, this approximation underestimates the actual result, and (hopefully) tends to offset the over-estimate due to the infinite-bounce approximation. In any case, both approximations get better as the disc gets thinner, since then even a ray starting near the edge takes many bounces to get to that edge, and the across-disc gain is low so even if a ray takes more bounces to exit than we calculate (due to greater reflectivity) the added radiation is small.

γ. Total Result

Adding together the results above and below the critical angle, we find that for low gain ($\alpha D \ll 1$ and $\alpha L \ll 1$) and thin discs we have

$$M \cong 1 + \alpha D \left(\frac{1}{2} - \frac{\theta_c}{\pi}\right)\left(\frac{1}{2} + G\right) + \alpha L \left(\frac{1}{T} - \frac{1}{2}\right) \ln\left(\frac{1}{\cos\theta_c}\right) \quad .$$

This result is for one value of $\alpha$, and thus corresponds to a flat line profile. Values of m corresponding to other line shapes may be calculated as in the sphere case.

With a Lorentzian line profile, the amplitude weighting function is $\rho_L(x) = \left[\pi\sqrt{x(1-x)}\right]^{-1}$. We can write M in the form $M = 1 + B\alpha(\lambda)$, where B is independent of $\lambda$. Then

$$M_L \cong \int_0^1 dx \; \frac{1 + B\,\alpha\,x}{\pi\sqrt{x(1-x)}}$$

$$= 1 + \frac{B\alpha}{\pi}\int_0^1 dx \; \sqrt{\frac{x}{1-x}}$$

$$= 1 + \frac{B\alpha}{\pi}\;\frac{\pi}{2}\,,$$

where $\alpha$ is now the gain coefficient at the line peak.

We thus have

$$M_L \cong 1 + \frac{\alpha}{2}\,B,$$

or

$$M_L \cong 1 + \alpha\,D\left(\frac{1}{4} - \frac{\theta_c}{2\pi}\right)\left(\frac{1}{2} + G\right) + \alpha\,L\left(\frac{1}{2T} - \frac{1}{4}\right)\ln\left(\frac{1}{\cos\theta_c}\right).$$

With a Gaussian line profile, $\rho_G = \left(\sqrt{-\pi\,\ln x}\right)^{-1}$ and we get

$$M_G \cong \int_0^1 dx \; \frac{1 + B\,\alpha\,x}{\sqrt{-\pi\,\ln x}}$$

$$= 1 + \frac{B\alpha}{\sqrt{\pi}} \int_0^1 dx \; \frac{x}{\sqrt{-\ln x}}$$

$$= 1 + \frac{B\,\alpha}{\sqrt{\pi}} \sqrt{\frac{\pi}{2}} \quad .$$

We thus have

$$M_G \cong 1 + \frac{\alpha}{\sqrt{2}} \; B,$$

or

$$M_G \cong 1 + \frac{\alpha D}{\sqrt{2}} \left(\frac{1}{2} - \frac{\theta_c}{\pi}\right)\left(\frac{1}{2} + G\right) + \frac{\alpha\, L}{\sqrt{2}} \left(\frac{1}{T} - \frac{1}{2}\right) \ln\left(\frac{1}{\cos\theta_c}\right) \quad .$$

Since the low-gain result in any geometry will always have the form $M = 1 + C\alpha$ or $A = C\alpha$ (where C is a constant depending on the geometry), the flat-topped, Gaussian, and Lorentzian lines will always have the low-gain ratios $2:\sqrt{2}:1$ exhibited for the sphere and cylinder.

2. Monte Carlo Calculation

ZAP was used to find the stimulated-spontaneous ratio A in circular discs. Again the inversion (and thus the gain coefficient) was assumed spatially uniform. The reflection at the face was taken as the average over polarization. In Fig. 8, we see the results for flat, Gaussian, and Lorentzian line profiles in discs whose thickness is 20% of their diameter.

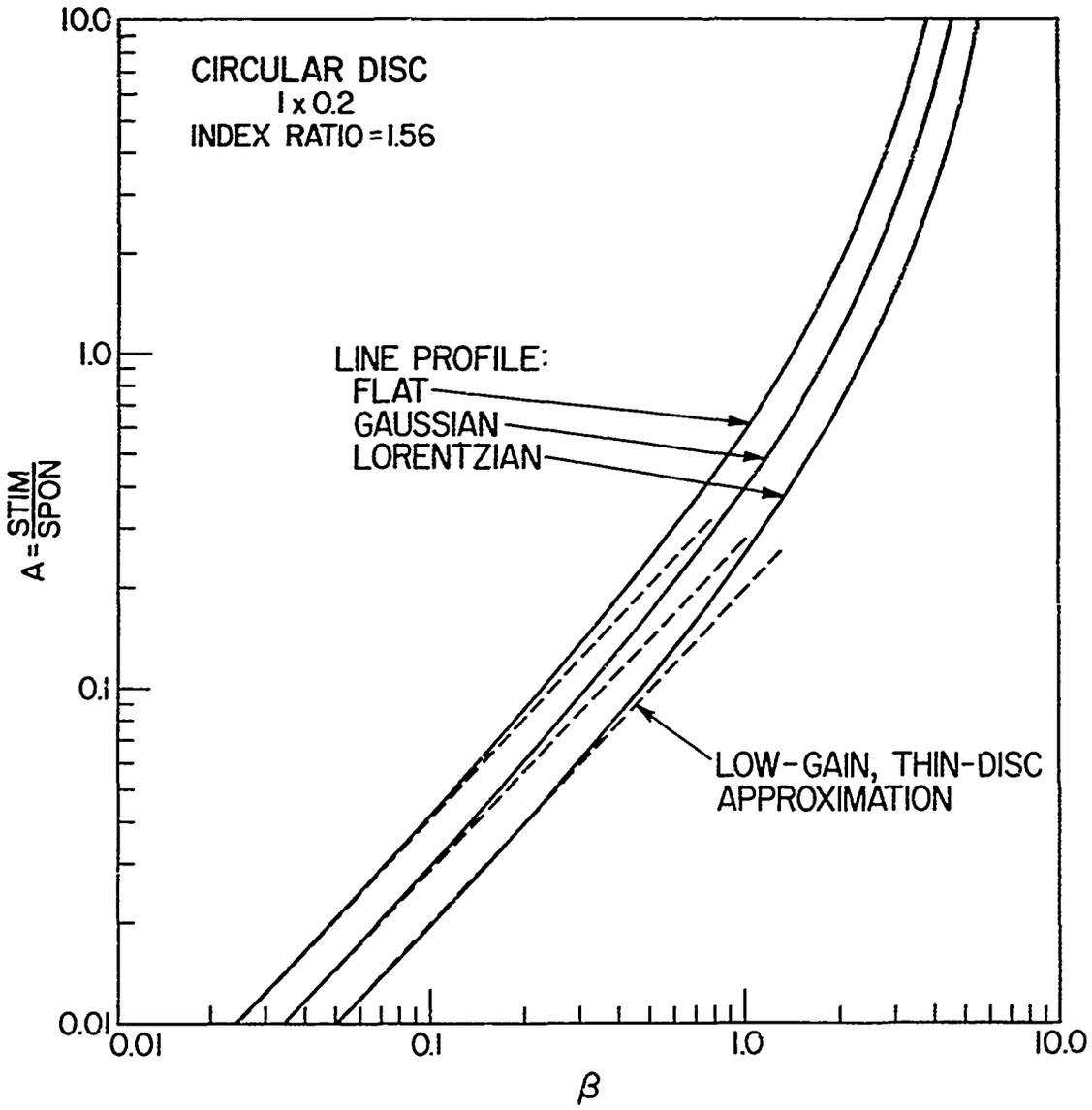


Fig. 8 - Monte Carlo values of the ratio A of stimulated to spontaneous loss as a function of the product β of the gain coefficient and diameter for a circular disc of thickness equal to 20% of its diameter. The ratio of the refractive index inside the disc to that outside the faces is 1.56. Curves are shown for three different line profiles of the gain coefficient. The low-gain, thin-disc approximation is shown for comparison.

The refractive index inside the discs was 1.56 times the index outside and the circular edge of the disc was totally absorbing. The A ratios are shown as a function of $\beta = \alpha D$, where $\alpha$ is the gain coefficient at the line peak and D is the disc diameter. Also shown is the small-gain, thin-disc approximation. The approximation is seen to be good below $\beta \cong .1$, even for discs this thick.

The A curves have the same general shape as the curves for a sphere, except for a faster rise when A is greater than one (this faster rise is due to the longer path available in the cylinder due to total internal reflection from the faces).

The amount of fluorescence amplification in a disc depends on the disc thickness and on the ratio of refractive indices inside and outside the sphere, as well as on the gain coefficient. As the cylinder index approaches the index of its surroundings, less and less of the light inside it undergoes total internal reflection, and A becomes lower. For exact index matching, no light returns into the disc and A has its minimum value. The variation of A with index ratio is shown in Fig. 9 for various values of $\beta$. The low-gain, thin-disc approximation is also shown in Fig. 9, and is seen to match the Monte Carlo results well except at low index ratios, where the angle for total internal reflection increases and the infinite-bounce approximation breaks down.

The Monte Carlo results for the variation of A with relative disc thickness are shown in Fig. 10. The values for $\beta = .1$ are compared to the low-gain, thin-disc approximation. The approximation is seen to be good to at least 80% disc thickness. The most interesting feature of these results

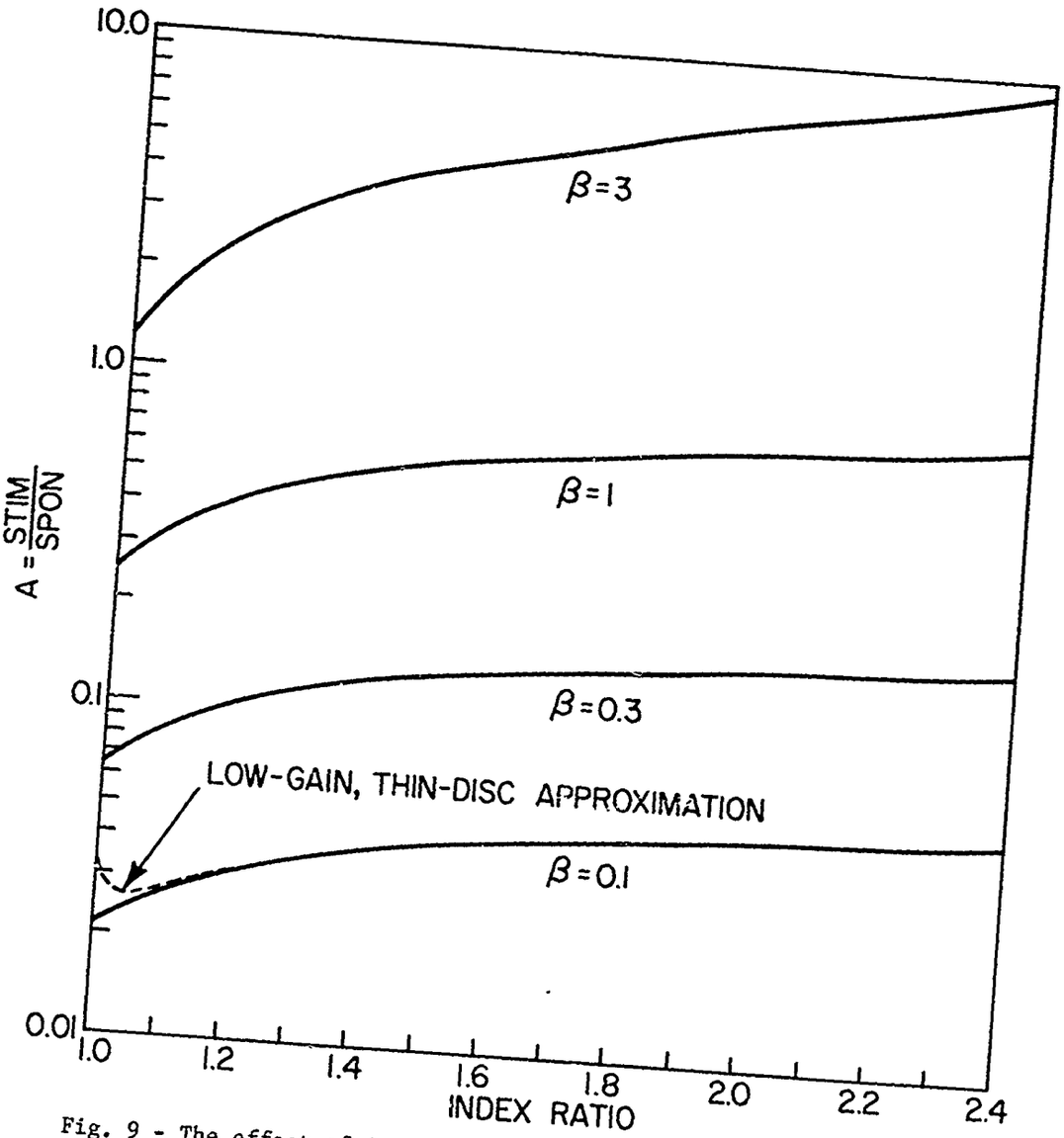


Fig. 9 - The effect of inside-outside refractive index ratio on the fluorescence amplification in a 20% thickness circular disc. The increase with index ratio is due to the greater fraction of radiation trapped by total internal reflection at higher ratio. The low gain, thin-disc approximation is compared to the $\beta = .1$ result, which it fits exactly except at low ratios.

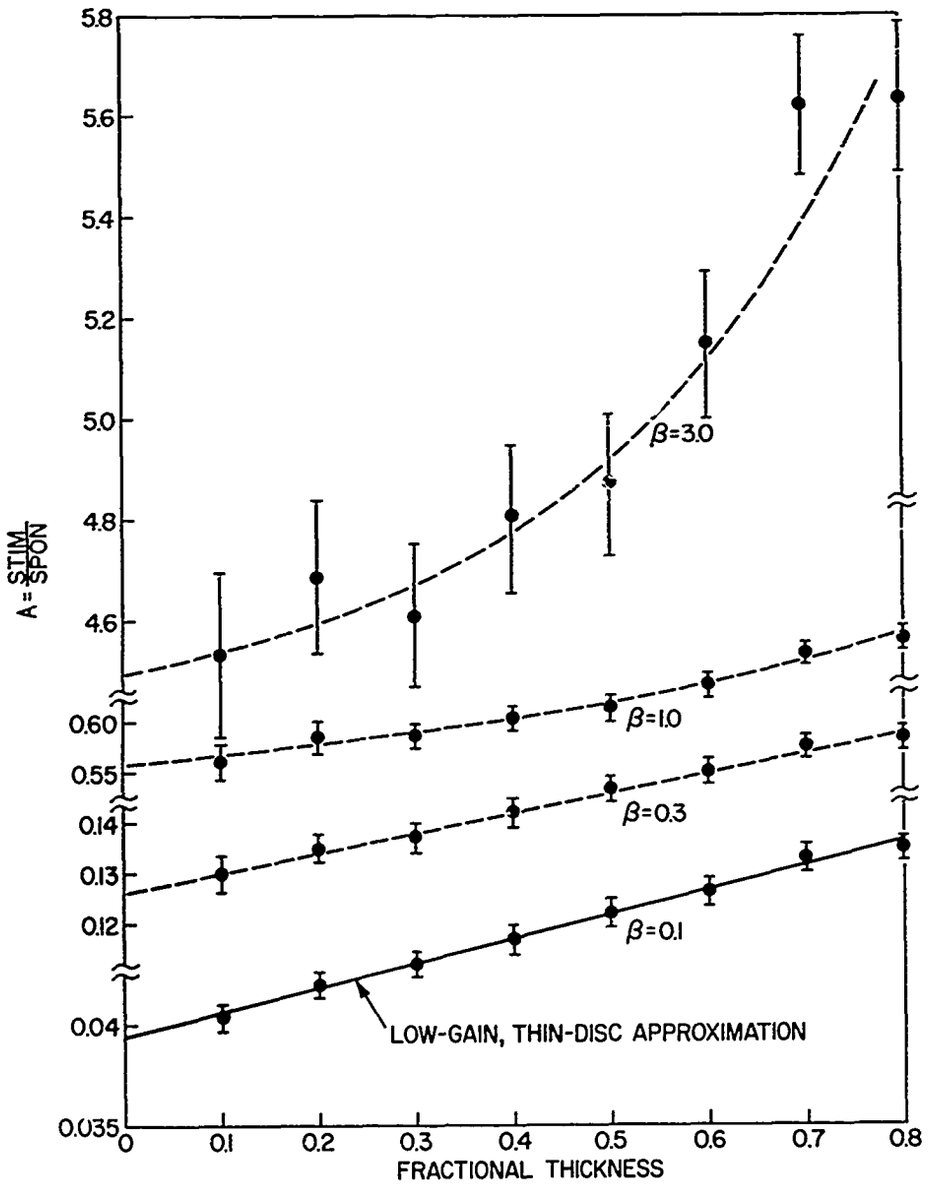


Fig. 10 - The fluorescence amplification in a disc of 1.56 inside-outside refractive index ratio as a function of the ratio of the disc thickness to its diameter. The increase is slow because the principal contribution is from rays undergoing total internal reflection, and this contribution is independent of thickness. The low-gain, thin-disc approximation is compared with the $\beta$ = .1 result. Note broken vertical scale.

is the very slow increase of fluorescence amplification with disc thickness. This slow increase arises because much of the fluorescence amplification in a disc is due to rays which are totally reflected at the faces of the disc, and the contribution of such rays is independent of disc thickness. Since useful laser gain is roughly proportional to disc thickness, discs should be as thick as possible within the constraints of pumping uniformity, thermal distortion, self-trapping, and fabrication difficulty. There is also an obvious advantage in trading a thick, weakly-doped disc for a thin, highly-doped disc, since fluorescent lifetime usually decreases with doping.

C. Elliptical Disc

Analytical computation is difficult in the case of an elliptical disc, and unnecessary in light of the good fit of the Monte Carlo results to the sphere and circular disc cases. Therefore only Monte Carlo calculations were made in this case. The computations were for discs whose major and minor axes were in the ratio 1:0.5, which is typical of laser glass tilted at Brewster's angle in air if the beam is round. The thickness was 1/7 of the major axis, since this corresponds to an actual disc in use in a multidisc laser amplifier in our laboratory. Once more, the inversion was uniform, the inside-outside refractive index ratio was 1.56, and the curved edge was totally absorbing.

The ratio of stimulated to spontaneous radiation, A, is shown in Fig. 11 as a function of $\beta = \alpha D$, where D is the disc major axis. The results are about 70% of those for a circular disc of diameter equal to the ellipse major axis, for low values of $\beta$. As $\beta$ increases, this fraction decreases.

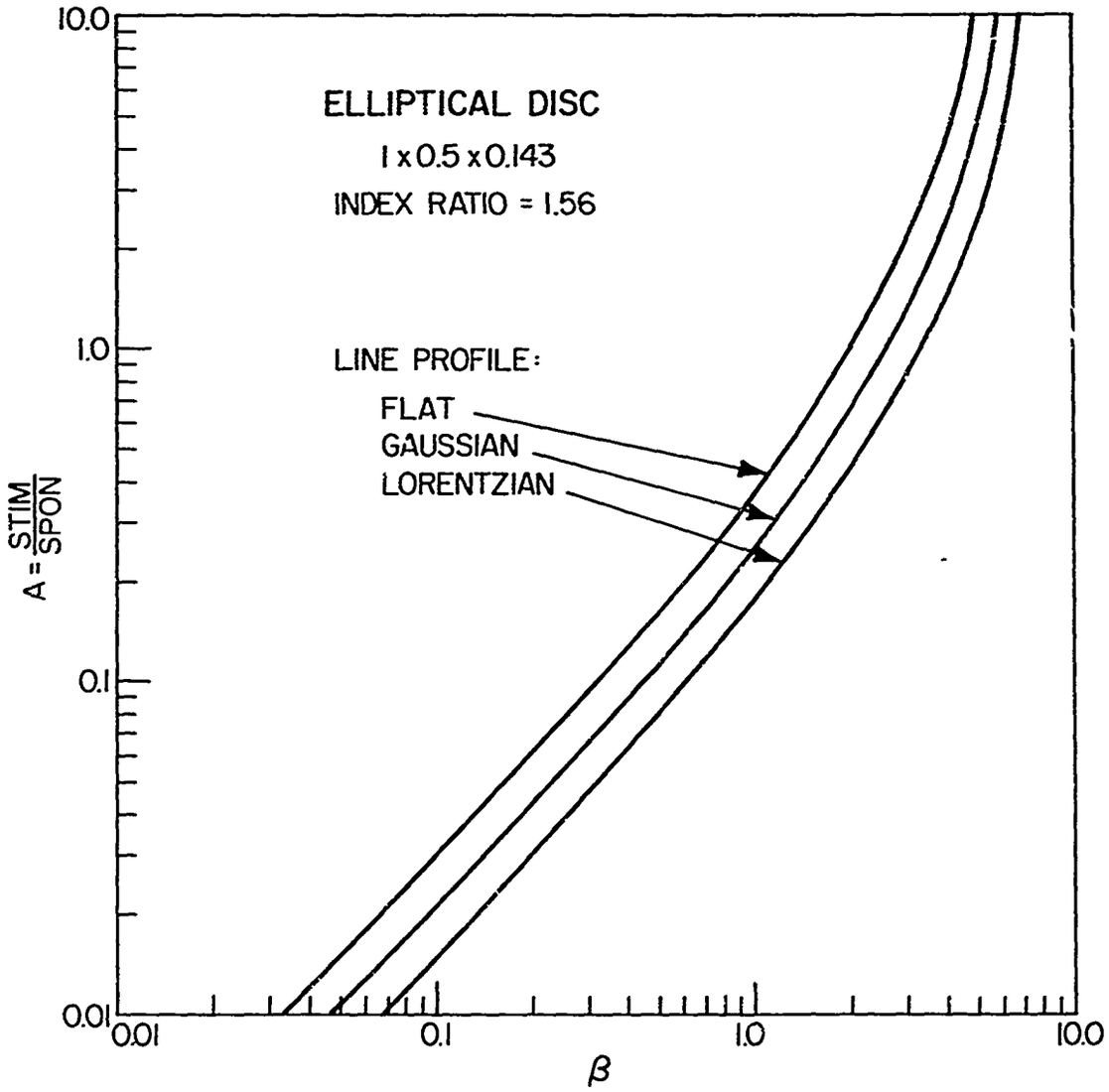


Fig. 11 - Monte Carlo values of the ratio A of stimulated to spontaneous loss as a function of the product β of the gain coefficient and major axis for an elliptical disc of minor axis 50%, and thickness 14.3%, of its major axis. The inside-outside refractive index ratio is 1.56. Curves are shown for three different line profiles of the gain coefficient.

The radiation absorbed by the disc edge and that exiting from the disc face were found separately in the elliptical disc calculations. These values are shown in Fig. 12 as a function of $\beta$. We see that the greater part of the stimulated radiation increase at high $\beta$ goes to the disc edge, rather than to the disc face. In high energy systems, the edge absorber may thus have to withstand large loadings.

D. Discussion

We have studied the problem of fluorescence amplification, in which the fluorescence emitted by a material with optical gain is amplified by stimulated emission as it passes through the material, thus increasing the natural fluorescent loss rate. We have defined the ratio of total loss to fluorescence M and the ratio of stimulated to spontaneous loss A.

Fluorescence amplification causes pumping to become more and more difficult as the stored energy (and thus the gain) increases in a material. In effect, the energy decays with an instantaneous fluorescent lifetime given by $\tau/M$, where $\tau$ is the natural or low-gain lifetime. This means that as the pump strength is increased, inversion will not increase in proportion. The resulting pump efficiency decrease is a slow function of the pump energy, rather than the abrupt upper limit due to parasitic oscillation (Section III). The exact details of the process depend on the geometry of the material and the fluorescent line shape, but in general pumping is quite difficult when the gain across the longest dimension of the material is about exp (5) $\cong$ 150 or more (we assume that the natural lifetime is not extremely long, so that its decrease by a factor of 10 is a serious problem). The effect of fluorescence amplification on pumping will be considered in detail in Section IV.

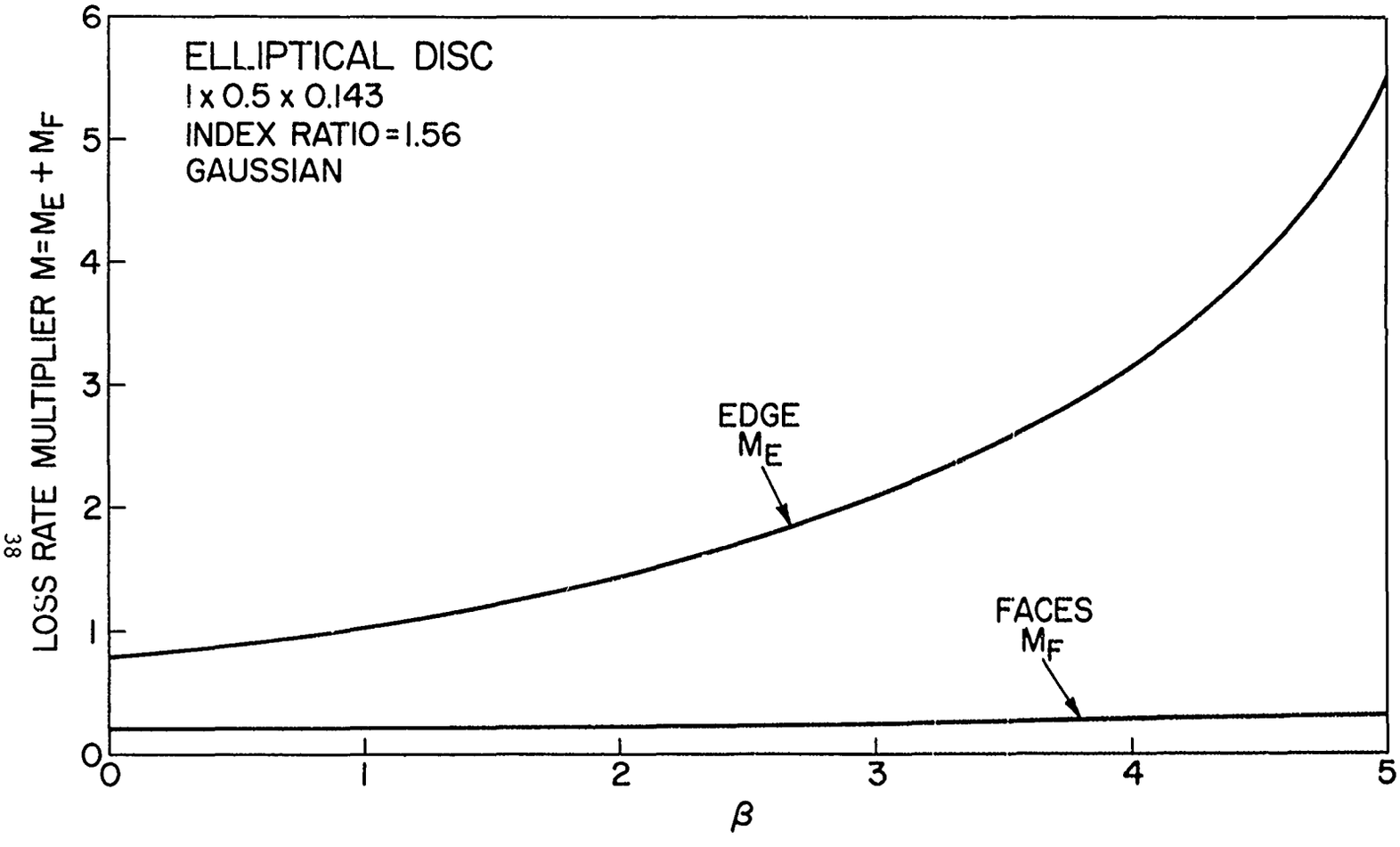


Fig. 12 - Amount of ratio M of total to spontaneous loss due to radiation absorbed at edge ($M_E$) and lost from faces ($M_F$) in an elliptical disc, as a function of $\beta$. Most of the increased loss due to fluorescence amplification is seen to go to the edge rather than out the faces.

The line shape of the fluorescent emission (and gain) is important because a line with broad, low wings has less fluorescence amplification than a more rectangular line, for the same peak value of the gain. For low gain, we have shown that the ratio A has the relative values $2:\sqrt{2}:1$ for flat (rectangular), Gaussian, and Lorentzian gain profiles; Monte Carlo calculations show that these relations are roughly maintained at higher gains. Actual laser materials often have complicated, multi-peaked line profiles, but in principle we could find the single-wavelength value $A_\lambda$ for the geometry we are using and then (perhaps numerically) integrate this with the amplitude weighting function corresponding to the laser material we are using. In practice, it is undoubtedly sufficient to estimate where in the flat-Gaussian-Lorentzian family the actual line shape lies and to interpolate to find A for that line shape.

The geometry of the amplifying material strongly influences the amount of fluorescence amplification. In the simple case of a sphere, A and M depend only on the product of the gain coefficient $\alpha$ and the disc diameter D, and of course on the line shape. When we consider a circular disc, we find that A and M depend not only on $\alpha D$, but also on the refractive index ratio between the inside and outside of the disc, and on the ratio of thickness to diameter of the disc. An index match between inside and outside is desirable since it leads to the least possible fluorescence amplification. However, in short-pulse high-power lasers the index-matching material may cause problems due to self-focusing damage, so this remedy is not always available. The fluorescence amplification is also least for vanishingly thin discs, but of course such discs have insufficient gain along the path of the actual laser pulse to even

overcome their own surface losses. Since the increase of fluorescence amplification with thickness is slow, it is not harmful to increase the disc thickness until it is limited by other considerations. For example, the deposition of pump energy changes with disc thickness, but this question is beyond the scope of this paper. An elliptical disc has the same type of index and thickness behavior as a circular disc, but the fluorescence amplification is somewhat less than in the circular case. Elliptical discs have the additional advantages of smaller size and hence lower cost (when compared to circular discs tilted at Brewster's angle to a circular beam) and closer coupling to the pump sources.

## III. PARASITIC OSCILLATION

Parasitic oscillation takes place when a material with optical gain has in it (or through it) a light path which returns on itself. Under this condition, the material will break into oscillation when the gain is large enough to overcome the path losses. Such undesired oscillation will make it impossible to increase the stored energy in the oscillating volume, since once oscillation begins all further pumping is immediately converted into oscillating power and lost. If the mode of oscillation fills an appreciable fraction of the laser volume, it thus sets a sharp upper limit to the available stored energy, and therefore the gain. If the mode gain does not vary greatly with frequency across the gain line profile (or if it oscillates so rapidly as to effectively sample all values of gain in the line), then the place where oscillation will begin is the line peak. This means that the maximum

gain coefficient $\alpha$ determines the oscillation threshold, so that rectangular line profiles are the best from the view point of parasitic oscillation, since they maximize the available laser output at the onset of oscillation.

Parasitic oscillation cannot be calculated by ordinary Monte Carlo methods, since the power in oscillating modes typically flows in precise directions at any point in space. Unless the Monte Carlo algorithm is lucky enough to start a ray at exactly the correct position going in exactly the correct direction, it will not find the mode at all. Imagine, for example, the simple case of two reflecting plane mirrors 1 cm in diameter spaced 10 cm apart, with a laser material between them. In the case of such large mirrors, we can ignore diffraction and do a simple ray-tracing analysis. The mode occupies the whole volume between the mirrors, so the Monte Carlo method just has to get the angle right. In fact, however, there is only one exactly correct direction - the direction perpendicular to the mirrors. Rays at a small angle from the correct direction will bounce between the mirrors a number of times before they miss a mirror and exit from the system. On the average, a ray at an angle $\epsilon$ from the system axis will bounce N times, where N is given by

$$N \cong \frac{d}{2\ell\epsilon}$$

where d is the mirror diameter and $\ell$ is the inter-mirror distance. If the Monte Carlo method starts rays at random in angle, the probability of getting N or more bounces from a ray is

$$p(N) \cong \left(\frac{d}{4N\ell}\right)^2 \quad .$$

The rapid decrease of p as N increases means that a very large number of rays must be started to get a ray with many bounces. For our 1 cm by 10 cm resonator, we must start 16,000,000 rays (on the average) to get one with 100 or more bounces. Clearly, random-starting ray-tracing methods are not suitable for mode finding unless considerable modification is made to them. Without such modification, a Monte Carlo algorithm may give what seem to be perfectly reasonable results even in the presence of an oscillating mode above threshold.

Since our Monte Carlo program is unsuitable for the analysis of parasitic oscillation, a simplified analytic method was used instead. The method uses a simple ray-tracing viewpoint which ignores diffraction effects. In addition, phase is ignored and only amplitude is considered. Both these simplifications are justified on the basis that typical discs used in large lasers are very much larger than a wavelength, so that modes have low diffraction loss and close spacing in wavelength.

We will first consider lossless modes which rely on total internal reflection, then modes which have some loss and thus require gain in the laser material to achieve threshold, and finally the effects of a rough disc edge on the mode threshold.

A. Lossless Modes in a Circular Disc

It is possible for a mode which is totally lossless to exist in a circular cylinder because all reflections are by total internal reflection.

Consider, for example, the disc shown in Fig. 13. The disc faces are in contact with a medium with refractive index $n_1$, the disc itself has index $n_2$, and the (smooth) edge of the disc is clad with an absorbing material of index $n_3$ (we ignore any imaginary component of the absorber index). If the edge coating index $n_3$ is less than $n_2$, then total internal reflection is possible off the inside of the disc edge, and a ray can bounce losslessly around the disc perimeter in a plane parallel to the faces (Fig. 14). In addition, if the outside index $n_1$ is less than the disc index $n_2$, a ray can bounce from face to face of the disc by total internal reflection (Fig. 15).

In general, a ray may bounce off both the faces and the edge, and the ray path will be complicated (Fig. 16). We can describe such a path in terms of two angles: $\Psi$ measures the angle of the ray from a disc diameter (Fig. 14), and $\theta$ measures the angle from a normal to the faces (Fig. 15). The angle of incidence on the faces is thus $\theta$, and the angle $\phi$ of incidence on the edge obeys $\cos\phi = \cos\Psi \sin\theta$. Thus as $\theta$ becomes smaller, $\phi$ becomes larger. For a ray to be lossless, we must have both $\theta > \theta_c = \sin^{-1}(n_1/n_2)$ and $\phi > \phi_c = \sin^{-1}(n_3/n_2)$. This dual condition sets a lower bound on $\Psi$, since we must have $\cos\Psi < \cos\phi_c/\sin\theta_c$. Thus we must have

$$\Psi \geq \cos^{-1}\left[\frac{n_2}{n_1}\sqrt{1-\left(\frac{n_3}{n_2}\right)^2}\right]$$

which implies that the lossless oscillation exists only outside a center portion of the disc of radius $R = D/2 \sin\Psi_o$, where $\Psi_o$ is the minimum value of $\Psi$.

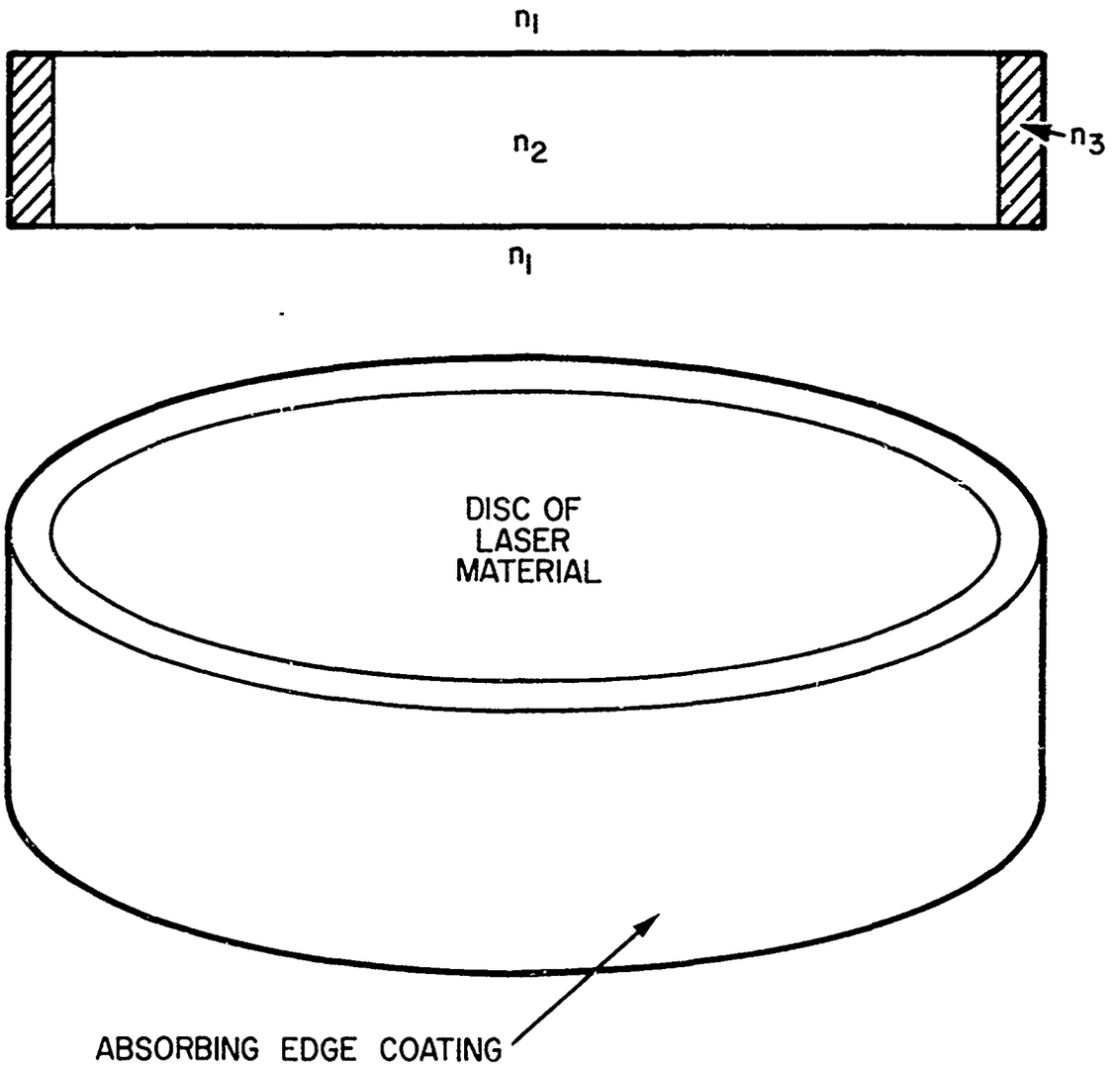


Fig. 13 - The disc configuration considered in the parasitic oscillation calculation. A circular disc of index $n_2$ is embedded in a material of index $n_1$. The edge of the disc is clad with an absorbing material of index $n_3$.

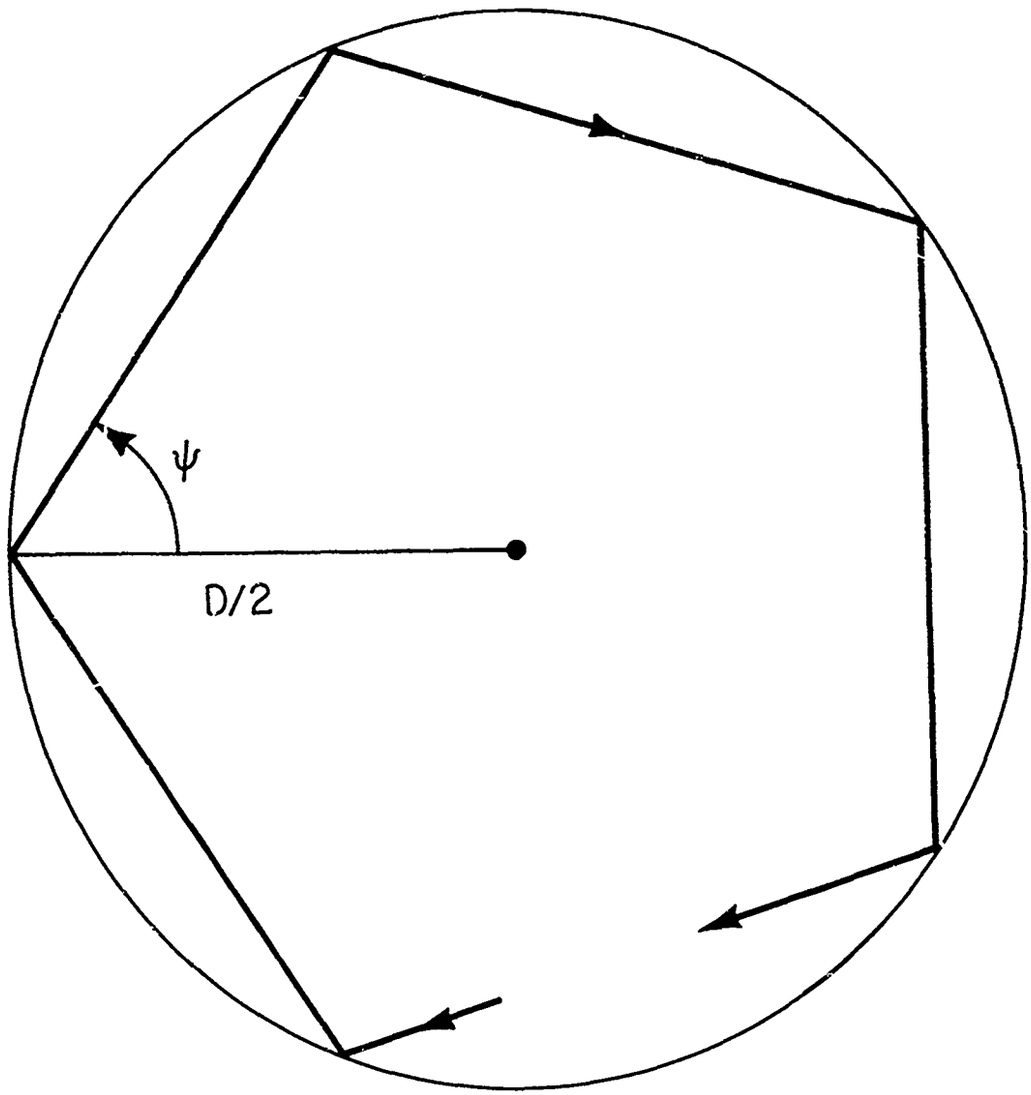


Fig. 14 - Typical lossless ray path possible if the disc index is greater than the edge-coating index. Total internal reflection takes place at the reflection points.

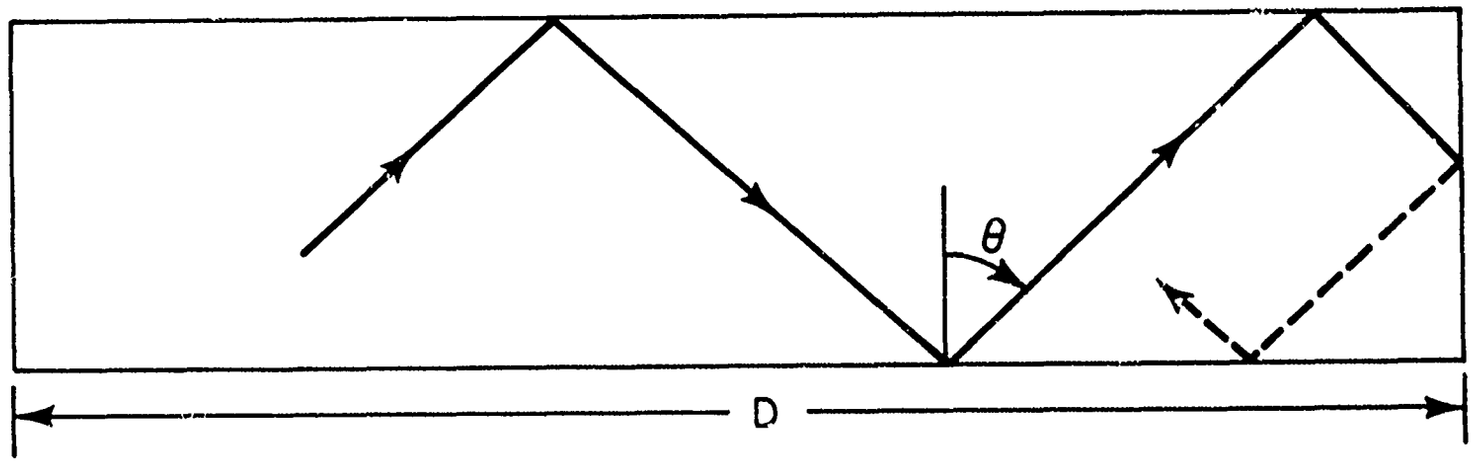


Fig. 15 - Typical ray path possible if the disc index is greater than the index of the surroundings. Total internal reflection takes place at the face reflections.

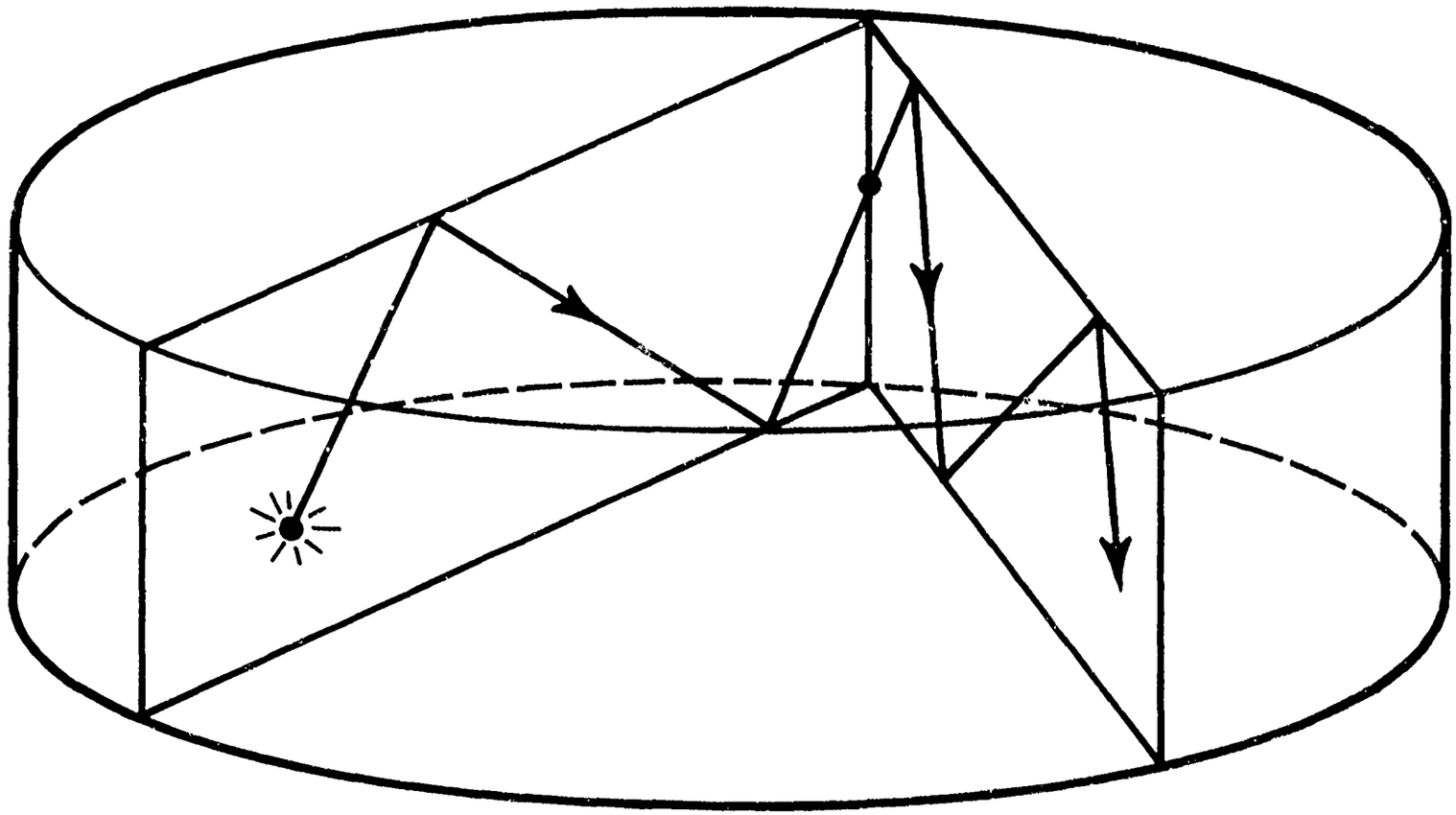

Fig. 16 - The path of a ray which bounces off both the faces and the edge. Between edge reflections, the path zig-zags in a plane perpendicular to the faces; the path changes to a new plane at each edge reflection.

We conclude that if the edge coating refractive index is less than the disc index lossless modes can exist in a circular disc. This means that as soon as there is any gain at all in the material oscillation will commence and further gain rise will be inhibited. The actual mode volume depends on the edge/disc and outside/disc refractive index ratios. It is clearly desirable to have the coating index larger than the disc index, since then lossless modes do not exist.

B. Lossy Modes in a Circular Disc

Even if there are no lossless modes in a disc, it will still oscillate on lossy paths if the gain is high enough. We wish to find the maximum gain achievable without parasitic oscillation, so we must find the mode with the least loss.

Consider a path which reflects off the disc faces by total internal reflection, but which has only partial reflection at the edge. We will use the same angles $\Psi$, $\theta$ as we used in the previous section to describe the ray. Let us assume that the edge reflection is given by $R_\sigma$, the larger of Fresnel's reflection coefficients. Then

$$R = \left[\frac{\sin(\phi - r)}{\sin(\phi + r)}\right]^2$$

where $r = \sin^{-1}(n_2/n_3 \sin\phi)$ and $\phi$, as before, is given by $\phi = \cos^{-1}(n_1/n_2 \cos\Psi)$ when $\theta$ is equal to $\theta_c$. The path length between edge bounces is $D \cos\Psi/\sin\theta_c = D\, n_2/n_1 \cos\Psi$, where D is the disc diameter. To oscillate, the net gain must be equal to unity, or

$$\left[\frac{\sin(\phi-r)}{\sin(\phi+r)}\right]^2 e^{\frac{\alpha D n_2}{n_1}\cos\Psi} = 1$$

where $\alpha$ is the gain coefficient at the line peak, $\phi = \cos^{-1}(n_1/n_2 \cos\Psi)$ and $r = \sin^{-1}(n_2/n_3 \sin\phi)$. We could now vary $\Psi$ in this expression to find the minimum $\alpha$ required for oscillation, but it is sufficient to examine the behavior at $\Psi = 0$ and $\Psi = \pi/2$. Solving for $\alpha D$, we have

$$\beta(\psi) = \alpha D = \frac{2n_1 \ln\left[\frac{\sin(\phi+r)}{\sin(\phi-r)}\right]}{n_2 \cos\Psi}$$

and

$$\beta(0) = 2\rho \ln\left(\frac{\sqrt{\sigma^2+\rho^2-1} + \rho}{\sqrt{\sigma^2+\rho^2-1} - \rho}\right)$$

where $\rho = n_1/n_2$ and $\sigma = n_3/n_2$, while

$$\beta(\pi/2) = \frac{4\rho^2}{\sqrt{\sigma^2 - 1}} \quad .$$

We have again used the variable $\beta = \alpha D$.

The calculation is only valid for $n_1 < n_2$ and $n_3 > n_2$, or $\rho < 1$ and $\sigma > 1$. In this region $\beta(0)$ is always less than $\beta(\pi/2)$, so we find that the lowest threshold modes are those in which the ray proceeds across a diameter of the disc, bouncing from face to face at the maximum angle which will produce total internal reflection. Such modes obviously fill the entire

disc volume. The threshold condition may be written

$$\beta_{CRIT} = \frac{2n_1}{n_2} \ln\left(\frac{\sqrt{n_1^2 - n_2^2 + n_3^2} + n_1}{\sqrt{n_1^2 - n_2^2 + n_3^2} - n_1}\right) .$$

Since the worst-case rays are those that travel diametrically across a circular disc, we expect the threshold for an elliptical disc of major axis equal to the disc diameter to be essentially the same as the circular threshold, since the same path is available. The surface curvature at the reflection points is of course larger in the elliptical case, but this should raise the threshold only slightly, since all it does is make the resonator somewhat more unstable.

In addition to the modes involving reflection off the edges, a relatively thick disc may also oscillate between its faces. The threshold for this process is easily calculated, since the face reflection at normal incidence is

$$R = \left(\frac{n_2 - n_1}{n_2 + n_1}\right)^2$$

and the gain from face to face is just exp ($\alpha L$), where L is the disc thickness. We must have R exp($\alpha L$) = 1, or

$$(\alpha L)_{CRIT} = 2 \ln\left(\frac{n_2 + n_1}{n_2 - n_1}\right) .$$

Of course, this result also applies to elliptical discs.

## C. Combined Oscillation Diagram

We may show the effects of both lossless and lossy modes on a single diagram in the $\rho$, $\sigma$ plane (recall $\rho = n_1/n_2$ and $\sigma = n_3/n_2$). When lossless modes fill the disc from a radius R outward, we use

$$\cos\psi = \frac{1}{\rho}\sqrt{1 - \sigma^2}$$

and

$$\sin\psi = \frac{2R}{D}$$

to derive

$$\left[1 - \left(\frac{2R}{D}\right)^2\right] \rho^2 + \sigma^2 = 1 \quad .$$

Thus the locus of constant R in the $\rho$, $\sigma$ plane is an ellipse. This result applies if $\rho < 1$ and $\sigma < 1$; if $\rho > 1$ then there is no total internal reflection off the faces and the answer becomes independent of $\rho$, since the oscillations lie in planes parallel to the disc faces and ignore the condition at the faces.

Lossy modes obey

$$\beta = 2\rho \ln\left(\frac{\sqrt{\sigma^2+\rho^2-1} + \rho}{\sqrt{\sigma^2+\rho^2-1} - \rho}\right) \quad ,$$

so we may draw loci of constant $\beta$ in the $\rho$, $\sigma$ plane to show how much gain may be achieved before oscillation commences. The lossy mode calculation is

valid if $\sigma > 1$ and $\rho > 1$, and again if $\rho > 1$ the expression becomes independent of $\rho$.

The diagram showing lines of constant oscillation-free radius R and lines of constant across-disc gain log $\beta$ is shown in Fig. 17. From the view point of oscillation suppression, the best place to operate is with both edge and face index-matched, since oscillation is impossible under these circumstances. If other considerations make such operation undesirable, the degree of oscillation difficulty encountered with other choices of refractive indices is easily evaluated from the diagram.

D. Parasitic Oscillation with a Rough Edge

Since the oscillatory modes considered above rely on rays which follow specific paths, one method of reducing oscillation tendency would seem to be the roughening of the disc edge, so that an initially parallel beam would be smeared out in angle. This ought to remove much of the energy from the mode, thus increasing the loss. However, energy will also be scattered into the mode from rays initially not involved. Clearly, a quantitative analysis of this situation is required. Again a Monte Carlo approach is inapplicable, since a ray which is randomly scattered at the edge has the same low probability of getting into the high-gain region of the mode as was the case with specular modes. Of course, we expect the active mode volume in space and angle to be larger with a rough edge than in the specular case, but the amount by which this helps the Monte Carlo method is hard to estimate.

The rough-edge oscillation was therefore analyzed by a method related to the well-known method of analyzing modes in an optical resonator. An

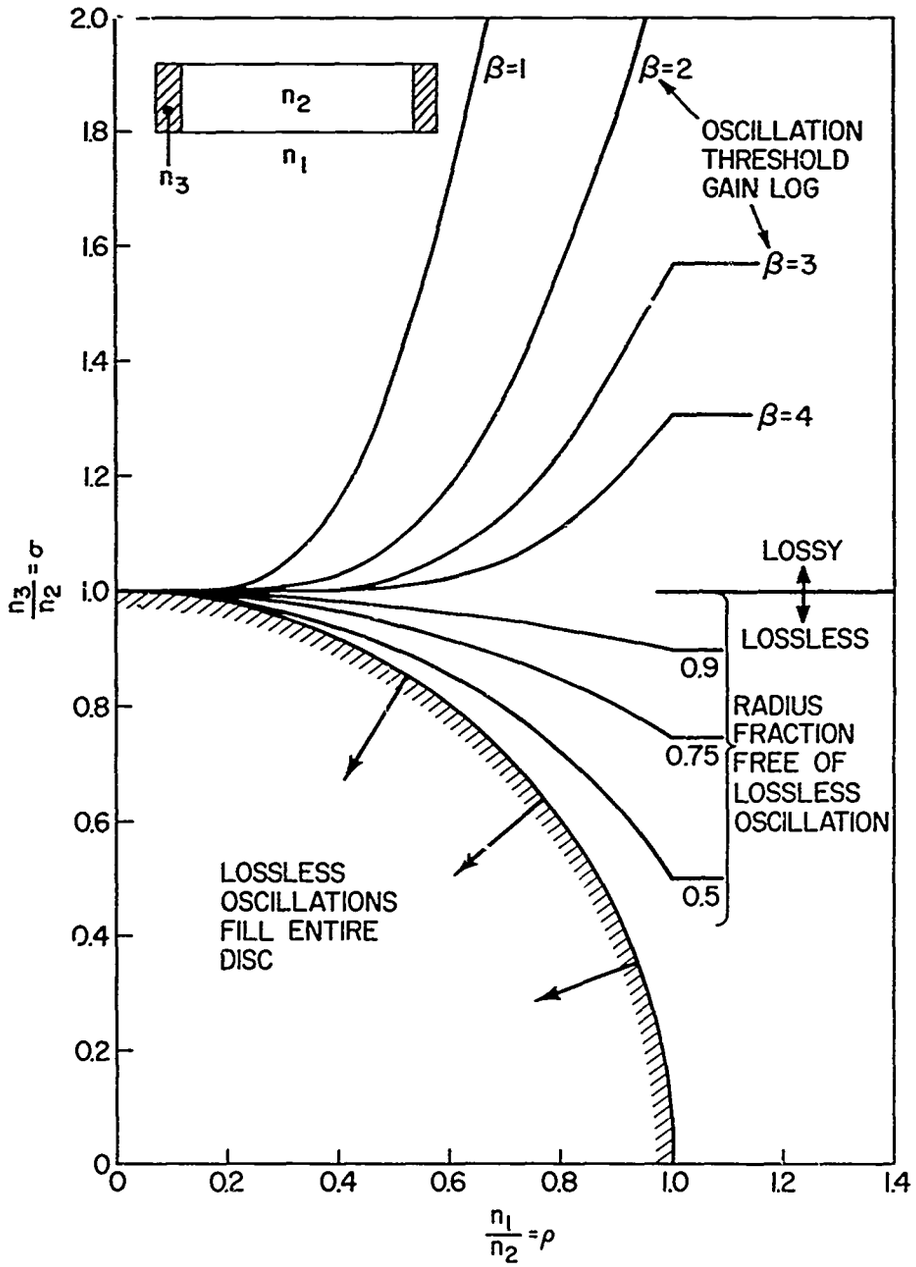


Fig. 17 - Combined diagram of lossless and lossy parasitic oscillation as a function of the index ratios of a circular disc. In the lower part of the diagram ($n_3/n_2 < 1$), the fraction of the disc free of lossless oscillations is shown. In the upper part ($n_3/n_2 > 1$), the $\beta$ required to commence oscillation along lossy paths is shown. See text.

initial angular distribution of optical power was assumed at the disc edge, and the power was then transported across the disc (with gain), reflected with loss, and scattered in angle. In general, the distribution after this process was different, in both amplitude and shape, from the original distribution. The gain coefficient was adjusted after each iteration to keep the amplitude constant, and the process was reiterated until the angular distribution of power had reached an equilibrium state. After many such iterations, the gain had the value appropriate to the oscillation threshold, and the angular power distribution was that of the oscillating mode. Once again, diffraction and phase were ignored.

Since radiation which is totally internally reflected from the disc faces has much higher gain travelling across the disc than radiation which is only partially reflected, the power was assumed totally lost when it was partially reflected. With this assumption, all points on the disc edge are equivalent, and only the angle of the optical power is important (as opposed to its position). The hemisphere of possible angles was divided into sectors of equal solid angle, and the resulting matrix of powers was iterated as above. The edge roughening was simulated by taking the unit vector along the direction of the reflected ray, and adding to it a random vector with uniform distribution throughout a sphere of radius $F \cos\theta$, where $F \leq 1$ and $\theta$ is the angle from the reflected ray to the normal. The resulting vector was then renormalized to unity. Various amounts of surface roughening were simulated by varying F from zero (specular reflection) to one (very rough). The edge reflectivity R was independent of angle.

The increase in threshold due to increasing F is shown in Fig. 18 for various values of the edge reflectivity. There is obviously improvement over the specular case, but it is not as great as might be expected. From a practical viewpoint, it is very hard to reduce the reflectivity of a rough surface to the low values achievable by index-matching a smooth surface, because of the many pits and cracks in a rough edge. Therefore one should be cautious when attempting laser improvements by edge roughening.

E. Discussion

We have shown that lossless modes exist for certain refractive index ratios between the inside, outside, and edge of a circular disc. Even if these modes are suppressed by proper choice of the indices, lossy modes will still exist. Such modes place an upper limit on gain, since once the gain reaches the mode threshold for oscillation, no further gain increase is possible in the mode volume. Highest gain is achieved for close index matching between the disc and the material in contact with its faces, and between the disc and the absorbing coating on its edge. We have shown what gain is possible if proper matching is not feasible for reasons not connected with oscillation.

Even if the absorbing material on the edge is a good index match to the disc, there may be areas of less-than-perfect adhesion, or chips and cracks in the disc edge. Such flaws will have reflection larger than the coating-disc interface, and in practice will make the achievement of very high absorption at the edge difficult. If the higher-reflectivity flaws are small,

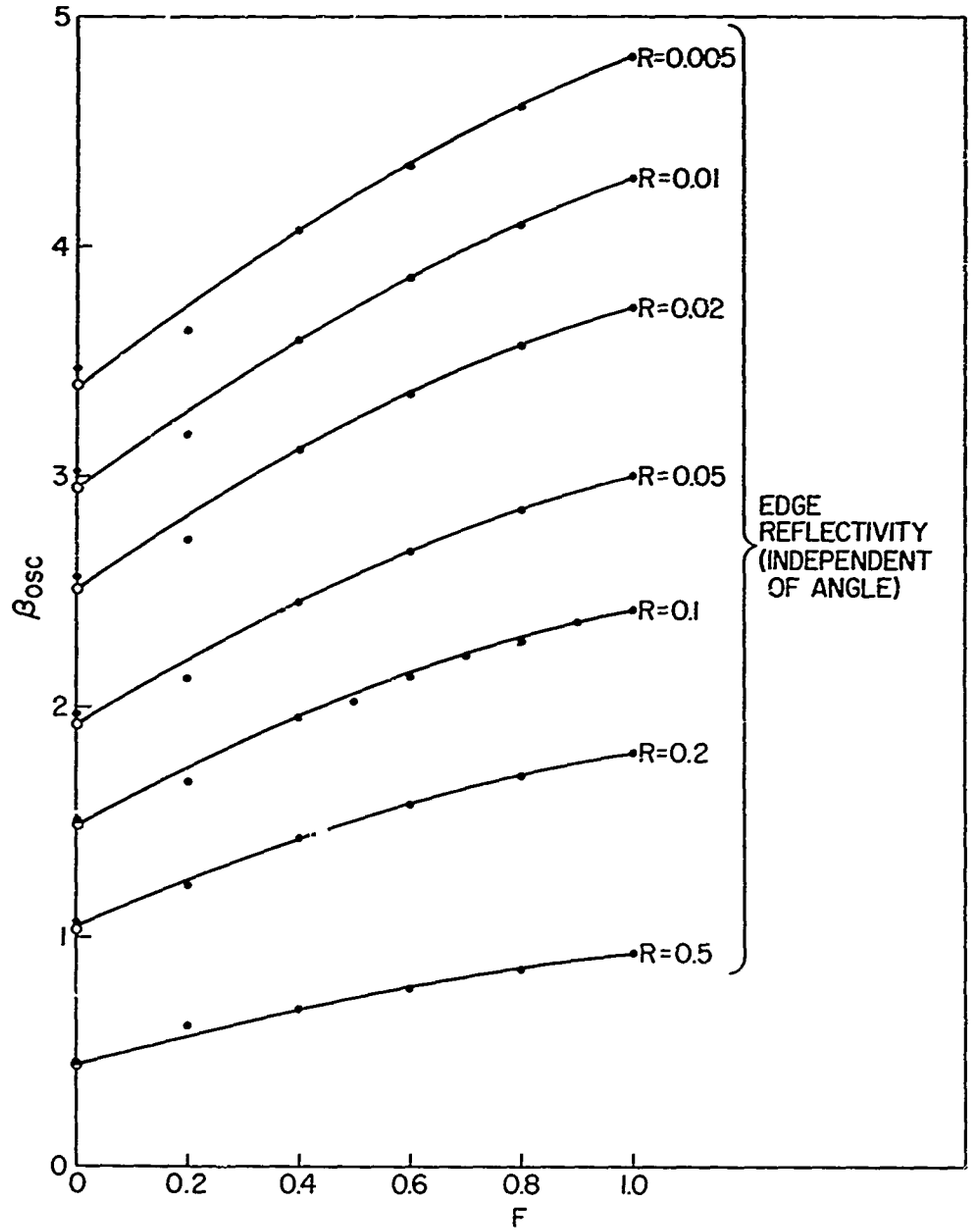


Fig. 18 - The moderate improvement in oscillation threshold achieved by various amounts of edge roughening. F is proportional to the amount by which the reflected rays are smeared out in angle about the specular direction.

diffraction will spread the reflected energy, but we have seen that such spreading causes only small threshold improvements. Thus a well-index-matched material must be applied extremely well to a flawless surface if a high parasitic oscillation threshold is to be achieved.

## IV. EFFECTS ON PUMPING

Our discussion so far has been confined to an instantaneous snapshot of the fluorescence amplification and parasitic oscillation processes. Lasers are usually pumped by relatively slow pump pulses, and we are interested in knowing what decrease in efficiency is caused by the loss processes we have calculated during such a pulse. We will first find the effect of fluorescence amplification, and then the effect of parasitic oscillation.

### A. Fluorescence Amplification

In the low-gain case, when fluorescence amplification is negligible, the stored energy decays with the fluorescent lifetime $\tau$. The gain has the same behavior, and so we may write a differential equation for the across-disc gain log $\beta$ in the form

$$\dot{\beta} = p(t) - \beta/\tau$$

where p(t) is the pump pulse (in appropriate units). At higher gain, fluorescence amplification increases the loss by a factor M, and so we have

$$\dot{\beta} = p(t) - \beta M(\beta)/\tau.$$

If we normalize to $\tau = 1$, and assume a half-sine approximation to the pump pulse, we get

$$\dot{\beta} = \frac{\pi\beta_o}{2T} \sin\left(\frac{\pi t}{T}\right) - \beta M(\beta) \qquad 0 < t < T$$

where $\beta_o$ is the area of the pump pulse and T is the base width of the pump pulse (in units of the fluorescent lifetime). In the range $0 \leq M \leq 5$, we may make a good approximation to M for any of the geometries and lineshapes studied by using the form

$$M \cong \exp\left(F\,\beta + G\,\beta^2 + H\,\beta^3\right).$$

Note that F may be found from the low-gain value of A, since $A \cong F\,\beta$ when $\beta \ll 1$. We may then find G and H by fitting a straight line to $(\ln M/\beta - F)/\beta = G + H\beta$.

Once M is approximated, we may integrate the differential equation for $\beta$ until it reaches its peak value. A plot of such maximum values is shown in Fig. 19 as a function of the pumping $\beta_o$, for various values of the pump pulse width. We see that fluorescence amplification is more serious for slow, large-area pump pulses while faster or smaller pulses suffer less loss. In the design of a flashlamp-pumped laser, the effects of current density on the pumping efficiency of flashlamps, and the effects of energy input on flashlamp life, should be integrated with this decay information in order to choose the optimum operating point.

Spatially uniform gain has been assumed in all our calculations of fluorescence amplification. However, the removal of energy due to

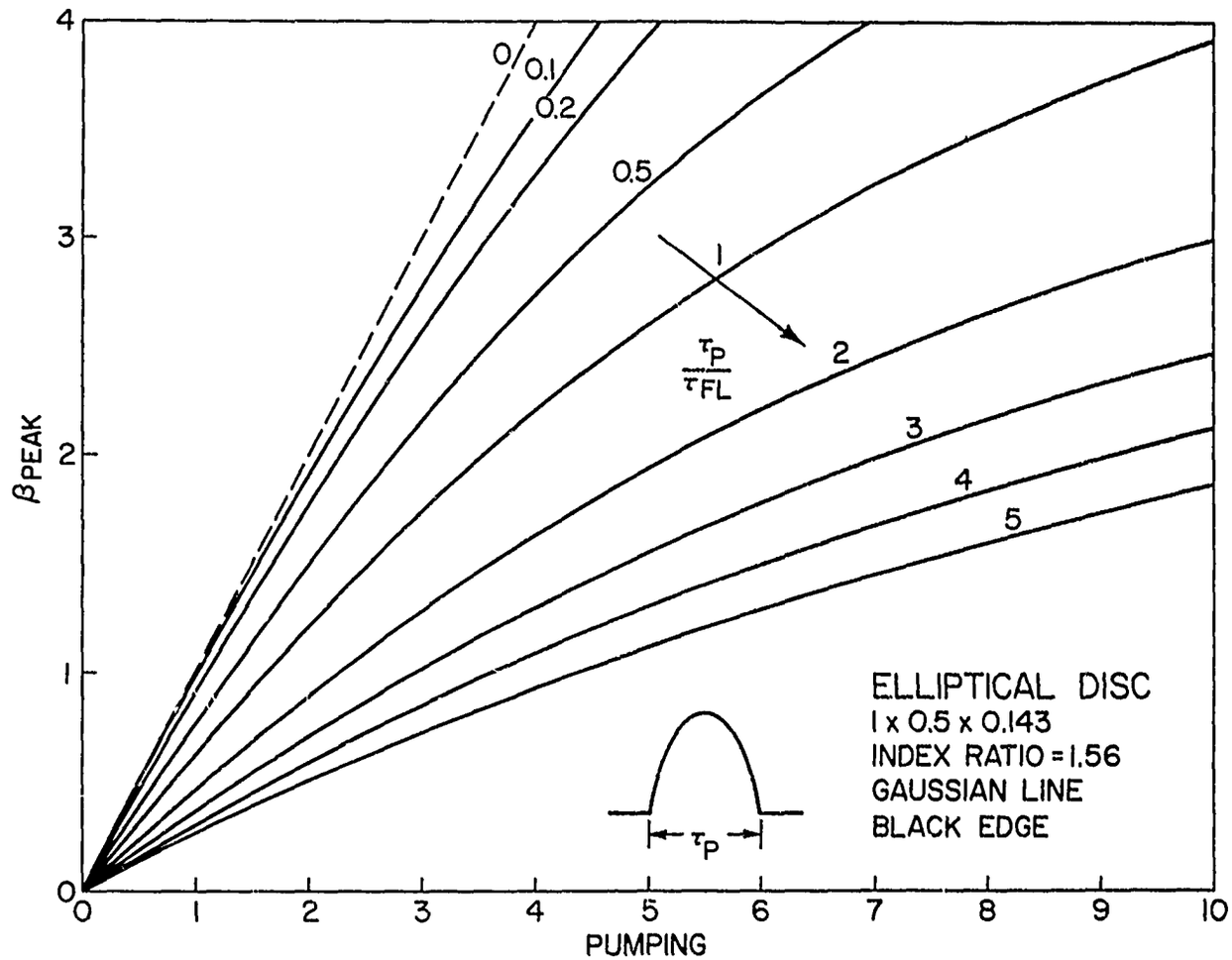


Fig. 19 - The maximum gain log β produced by half-sine pump pulses of various durations as a function of the pulse area. Since the inversion is proportional to β, this shows the achievable inversion for various ratios of pump width to fluorescent lifetime as a function of effective pump energy.

fluorescence amplification will be spatially non-uniform in general. Thus the gain will become non-uniform during a pumping pulse even if the pumping is uniform. The analysis of this problem is beyond the scope of this paper, but it is clear that proper tailoring of the spatial distribution of the pump energy can reduce or eliminate the difficulty.

B. Parasitic Oscillation

Parasitic oscillation causes a rapid limitation of stored energy, rather than the slow limitation we have seen above for fluorescence amplification. This is because a mode below its oscillation threshold contributes little to the loss rate, but once the mode is over threshold the loss rate is equal to the energy input rate. Thus the gain is sharply limited at the oscillation threshold. Figure 20 shows again the curve of gain versus pump area for a pump pulse of base width equal to the fluorescent lifetime, and also shows the type of gain saturation expected from the onset of oscillation. The oscillation threshold is shown for various ratios of the refractive index of the disc edge coating to the refractive index of the disc; this ratio determines the reflectivity at the edge. We have again assumed a disc-to-environment index ratio of 1.56. This diagram illustrates that unless very good index matching (or other reflection suppression) is used, parasitic oscillation will limit available energy storage well before fluorescence amplification losses become appreciable.

## V. CONCLUSIONS

The effects of fluorescence amplification and parasitic oscillation on laser energy storage and pumping efficiency have been analyzed. Fluorescence

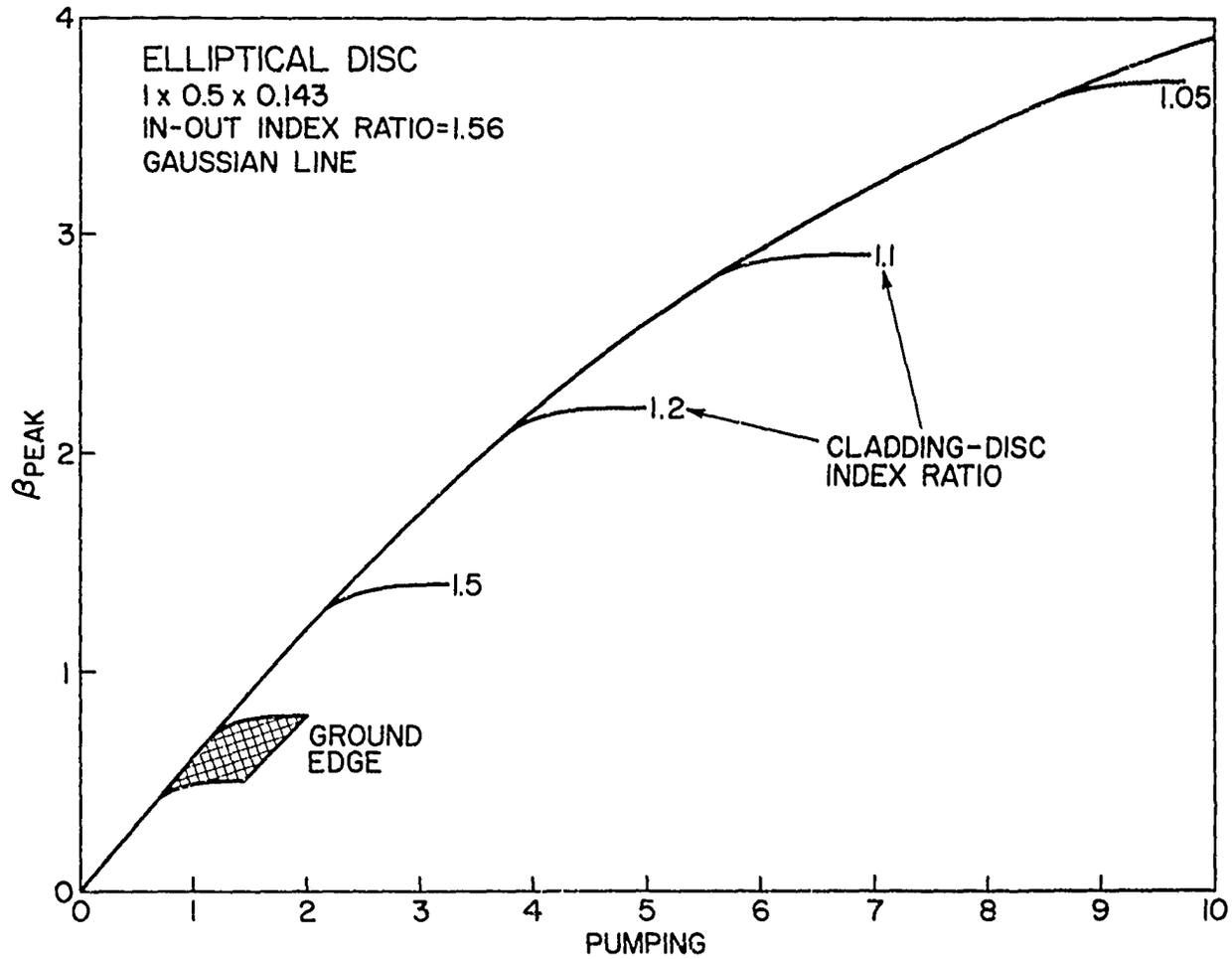


Fig. 20 - Parasitic oscillation limits shown on one of the pumping effectiveness curves of Fig. 19. The limitation gets more severe as the edge cladding index mismatch increases. Also shown are experimental limits for fine-ground, acid-etched disc edges.

amplification sets no definite upper limit on stored energy, but instead makes pumping more and more difficult as the energy density rises. Parasitic oscillation, on the other hand, sets an abrupt upper limit to stored energy at the oscillation threshold.

Fluorescence amplification is minimized by index-matching the material in contact with the faces of a laser disc to the refractive index of the disc. Increasing the disc thickness causes only a slow increase in the amount of fluorescence amplification, so thicker discs are of value if pump uniformity and thermal distortion limits are not exceeded.

Parasitic oscillation will occur at very low gain levels if the edge cladding material has a lower refractive index than the disc material. If this error is avoided, the level at which oscillation occurs will be maximized if the cladding index is as close as possible to the disc index. In addition, index-matching the faces raises the oscillation threshold. Roughening of the edges does not cause a great increase of the oscillation threshold, and may increase the average reflectivity of the edge, thus doing more harm than good.

What limitations do fluorescence amplification and parasitic oscillation place on glass laser amplifier disc size? Figure 20 shows that parasitic oscillation is the worst problem. Unless stringent precautions are taken, oscillation will set in at an across-disc gain of exp(3) or less, assuming the disc is in air to avoid self-focusing problems. With .5 J $cm^{-3}$ stored, the line-peak gain will be on the order of .1 $cm^{-1}$. This implies a 30 cm disc at most. This value will vary with stored energy and the amount of gain per

unit stored energy, but values much smaller than those quoted increase the amount of energy lost to the fixed loss coefficient in the glass. Thus operation with discs of dimension larger than about 30 cm will be very difficult, and operation in the 30 cm region will require great care in edge treatment to suppress parasitic oscillations.

## REFERENCES


1. W.R. Sooy, R.S. Congleton, B.E. Dobratz, and W. King, in Quantum Electronics - Proceedings of the Third International Conference, Vol. 2, Columbia University Press, New York, 1964, p. 1103.

2. L. Tonks, J. Appl. Phys. 35, 1134 (1964).

3. Yu. A. Anan'ev, A.A. Mak, and B.M. Sedov, Sov. Phys.-JETP 21, 4 (1965).

4. B.A. Ermakov, A.V. Lukin, and A.A. Mak, Opt. Spectrosc. 18, 201 (1965).

5. J.A. Fleck, Jr., J. Appl. Phys. 36, 1301 (1965).

6. Yu. A. Anan'ev, I.F. Balashov, and A.A. Mak, Sov. Phys.-Dokl. 11, 124 (1966).

7. E. Sibert and F. Tittel, J. Appl. Phys. 40, 4434 (1969).

8. A.A. Mak, B.G. Malinin, V.A. Novikov, D.S. Prilezhaev, A.I. Stepanov, and V.I. Ustyugov, Sov. Phys. - Tech. Phys. 14, 1418 (1970).

9. G.I. Peters and L. Allen, J. Phys. A: Gen. Phys. 4, 238 (1971).

10. L. Allen and G.I. Peters, Phys. Letters 31A, 95 (1970).

11. C.G.B. Garrett, W. Kaiser, and W.L. Bond, Phys. Rev. 124, 1807 (1961).